D317 CRUISE REPORT

Sea Spray, Gas Fluxes and Whitecaps Study (SEASAW)
Cruise D317 : March 21 – April 12 2007

Ian M. Brooks

October 2007

Institute for Atmospheric Science
School of Earth and Environment
University of Leeds
Leeds, LS2 9JT

Phone: 0113 343 6743
Fax: 0113 343 6716
Email: i.brooks@see.leeds.ac.uk

surface ocean solas lower atmosphere study
SEASAW

CONTENTS

DISCLAIMER

All data in this Cruise Report are provisional; some are fully calibrated, most are not. No data from this report should be published or otherwise presented without the express permission of the originators (see **Individual Scientific Reports**). The full data set will eventually be lodged with the British Oceanographic Data Centre (BODC).

ACKNOWLEDGEMENTS

We would like to thank the ship's Master, Roger Chamberlain along with all of the officers, engineers, and crew of the RRS Discovery for their support during cruise D317; it was a pleasure working with them. Steve Smith (CPO, Science) is especially thanked for his assistance with both the planning and execution of the buoy deployments.

The technical support of NMF-Sea Systems' staff Martin Bridger, Leighton Rolley, and Alan Shearing during the cruise is gratefully acknowledged. The assistance of Jon Short, Emma Northrop and Jason Scott made the cruise planning process a remarkably smooth one.

The logistical support provided to all the SOLAS cruises by Malcolm Woodward and Julia Crocker at PML was greatly appreciated – it lifted a huge burden of paperwork from the PI's shoulders freeing time to deal with scientific issues.

SEASAW is funded by the Natural Environment Research Council, under grant number NE/C001842/1, as part of the UK contribution to the international Surface Ocean Lower Atmosphere Study (SOLAS).

INTRODUCTION

Cruise number D317 of the RRS Discovery took place between March 21 and April 12 2007 in the NE Atlantic; sailing from Govan and returning to port in Lisbon. The primary region of scientific operations were between 57º and 60ºN, 15º and 23ºW, and at 50ºN, 22º to 26ºW with some additional measurements being made on the final transit to Lisbon. The sole scientific project undertaken was the Sea Spray, Gas Fluxes and Whitecaps Study (SEASAW).

The primary objectives of the cruise were to make measurements of the physical exchange of aerosols and trace gases (CO2 and ozone) across the air-sea interface under conditions of moderate to high winds, and to characterize the effects of the processes governing the exchange rates, in particular the influence of whitecaps. The main scientific goals of SEASAW are to:

- Establish the impact of various forcing parameters on the transfer velocities of CO_2 and O_3, and improve their parameterisation. These transfer velocities will be related to the transfer velocity of other trace gases via the Schmidt number.
- Determine the sea spray source function via direct eddy-covariance methods using ultrasonic anemometers alongside fast-response optical particle counters and condensation particle counters.
- Investigate wave breaking and whitecap production coincident with air-sea flux measurements, in order to provide increased understanding and improved parameterisation of wave breaking and whitecap production which is related to the observed air-sea fluxes.
- Investigate the production and fate of sea spray aerosol particles very close to the ocean surface by means of 10Hz optical particle counter observations with sub-surface bubble observations.
- Utilise a single particle aerosol mass spectrometer and associated instruments to study the composition of individual aerosol particles as a means of source apportionment and to investigate interactions between the sea spray aerosol and other aerosol and gaseous components

PROJECT PARTICIPANTS

Cruise science party:

Dr Ian Brooks[1] (SEASAW project PI and D317 PSO) i.brooks@see.leeds.ac.uk
Dr Sarah Norris[1] (PDRA) s.norris@see.leeds.ac.uk
Dr Justin Lingard[1] (PDRA) j.lingard@see.leeds.ac.uk
Mr Paul Smith[1] (PhD student) p.smith@see.leeds.ac.uk
Mr Anthony Bloom[1,5] (MRes Student)

Project collaborators:

Prof Michael Smith[1] (SEASAW CoI) m.smith@see.leeds.ac.uk
Dr Jim McQuaid (SEASAW CoI) j.mcquaid@see.leeds.ac.uk
Dr Barbara Brooks[1] b.brooks@see.leeds.ac.uk
Dr Margaret Yelland[2] mjy@noc.soton.ac.uk
Dr Ben Moat[2] bim@noc.soton.ac.uk
Mr Robin Pascal[2] rwp@noc.soton.ac.uk
Dr Meric Srokosz[2] (SEASAW CoI) mas@noc.soton.ac.uk
Dr David Woolf[3] david.woolf@thurso.uhi.ac.uk
Prof Gerrit de Leuuw[4] g.d.leeuw@hotmail.com

[1.] University of Leeds
[2.] National Oceanography Centre, Southampton
[3.] University of the Highlands and Islands, Scotland
[4.] University of Helsinki, Finland / TNO, Netherlands
[5.] Now at University of Edinburgh

NMF Support Staff:

Martin Bridger (computer support)
Leighton Rolley (computer support)
Alan Shearing (Engineering support)

Ship's Crew:

Roger Chamberlain (Master)
Richard Warner (Chief Officer)
Phil Oldfield (Second Officer)
Malcolm Graves (Second Officer)
George Parkinson (Chief Engineer)
Steve Bell (Second Engineer)
Alan Stevenson (Third Engineer)
Ian Collin (Third Engineer)
Robert Masters (Electrician)
Matthew Sangster (Motorman)

Mike Drayton (CPO Deck)
Steve Smith (CPO Science)
Ian Thompson (PO Deck)
Mark Moore (Seaman 1A)
Eric Downie (Seaman 1A)
Gerry Cooper (Seaman 1A)
Jason Marsden (Seaman 1A)
David Harthorne (Purser Catering Officer)
Peter Lynch (Head Chef)
William Isby (Chef)
Jeffrey Osborne (Steward)

SCIENTIFIC BACKGROUND

SEASAW has two distinct, but closely related goals: to determine the exchange rate of CO_2 across the air-sea interface and to determine the rate of production of sea-spray generated aerosol.

Determining the rate of exchange of trace gases across the air-sea interface is of paramount importance to climate. A large proportion of anthropogenic CO_2 is absorbed from the atmosphere by the oceans, of which approximately 60% is absorbed by the Atlantic Ocean (Takahashi et al., 1997). This net uptake is the result of a complex pattern of spatially and temporally varying source and sink regions.

Global carbon cycle models rely on CO_2 gas transfer velocity parameterisations to obtain global estimates of the oceans' CO_2 uptake. The parameterisations show an increase in CO_2 gas transfer velocities with increasing wind speed (e.g. McGillis et al. 2001), but show a scatter between studies of at least a factor of two. Very few direct measurements of CO_2 gas transfer velocities have been made at wind speeds exceeding $10ms^{-1}$ and as a result the parameterisations at high wind speeds diverge substantially and become even more uncertain. Although the past several years have seen substantial advances in our understanding of air-sea gas exchange these are still insufficient to adequately parameterise the fundamental controlling processes. For some gases, such as CO2, this is now the dominating uncertainty in global budgets.

Sea spray is an especially important aerosol because, with the exception of dust, it is the largest single source of aerosol mass injected into the atmosphere (Hoppel et al., 2001). When sea spray is produced at the ocean's surface, heat and water mass, plus associated chemicals, bacteria and viruses, are transferred from the ocean to the atmosphere. The transfer of heat, water vapour and momentum across the air–sea interface is crucial because of their influence on the intensity of tropical cyclones (Andreas and Emanuel, 2001). Over the open oceans sea salt aerosol are the dominant scatterer of incoming solar radiation (Haywood et al. 1999) and can modify marine stratocumulus clouds – one of the largest sources of uncertainty in climate predictions. Sea salt plays a significant role in marine stratocumulus microphysics and chemistry (O'Dowd et al. 1999), and can also provide a substantial sink for atmospheric trace gases, both natural and man made (O'Dowd et al. 2000).

At present there are substantial variations – roughly 5 order of magnitude for micron sized particles – in the values of the SSSFs available in the literature as a function of wind speed. Wind speed is the dominating controlling factor to the production sea spray aerosols however there are other variables such as, wind history, sea-state, the presence of organics and surfactants, water temperature, gas saturation, rain, surface-layer stratification – all of which are poorly understood. It is difficult to determine the extent to which the differences in the SSSF are influenced by sampling location or the range of meteorological conditions, such as wind speed. Measurements have typically suffered from a high degree of uncertainty and the challenge of obtaining direct observations near the air-sea interface at high sea states; these confounding effects have made the determination of empirical SSSFs difficult.

The fluxes of both aerosols and gases across the air-sea interface depend strongly on the turbulent wind stress at the surface. Although many existing gas exchange parameterizations that relate the gas transfer velocity (*kw*) solely to mean wind speed are widely used for data interpretation and in modelling, observational and theoretical evidence show such descriptions to be incomplete; air-sea exchange depends in a complex fashion on many additional factors, including wave state, the presence of surfactants, and the relative direction of wind and swell. Whitecaps and bubble bursting also directly influence aerosol generation and gas transfer. Very different values of *kw* may therefore be expected at different locations at identical wind speeds. Significantly improving the existing parameterizations requires that the second order effects be included. *SEASAW* aims to address some of these issues by including measurements of wave state, whitecap coverage, and bubble populations. The aim is to significantly reduce the uncertainties, particularly at high wind speeds where measurement is most difficult, and where the available data are most limited.

MEASUREMENT PROGRAMME

The primary aim of SEASAW was to make direct eddy measurements of air-sea fluxes under high wind speeds. The optimal sampling strategy is to have the ship stationary, hove-to with the mean wind direction maintained within 30 degrees of the bow. To this end we undertook measurements over periods of up to several days while remaining on station at a fixed location (see cruise maps), relocating when necessary to follow the changing weather systems. Almost all instrumentation operated continuously throughout the cruise, both when on station and during transits. When on station we deployed a small aerosol buoy on a more or less daily basis, for periods of several hours at a time (see science reports).

The short interval between the ill-fated D313 and D317 resulted in insufficient time being available to service some instrumentation damaged during D313, so that the background aerosol measurements are incomplete for D317.

INSTRUMENTATION SUMMARY

Foremast turbulence systems

The Leeds turbulence system consisted of:

- *Gill R3A sonic anemometer*: 3 components of turbulent wind and 'sonic' air temperature at 20Hz.
- *LiCOR-7500 open path gas analyzer*: water vapour and carbon dioxide concentrations at 20Hz. Located ~0.5 m aft of sonic anemometer sample volume.
- *CLASP aerosol probe*: 16 channel aerosol size spectra, 0.05-3.5 μm radius, at 10Hz. Inlets located next to LiCOR. Lag time from inlet to sensor head is approximately 2 sample intervals.
- *motion pack*: Centre of measurement relative to anemometer measurement volume: Δx = -0.808 m, Δy = -0.183 m, Δz = -0.668 m.
- *FLOS ozone sensor*: ozone concentration at 20Hz, inlets situated next to LiCOR.

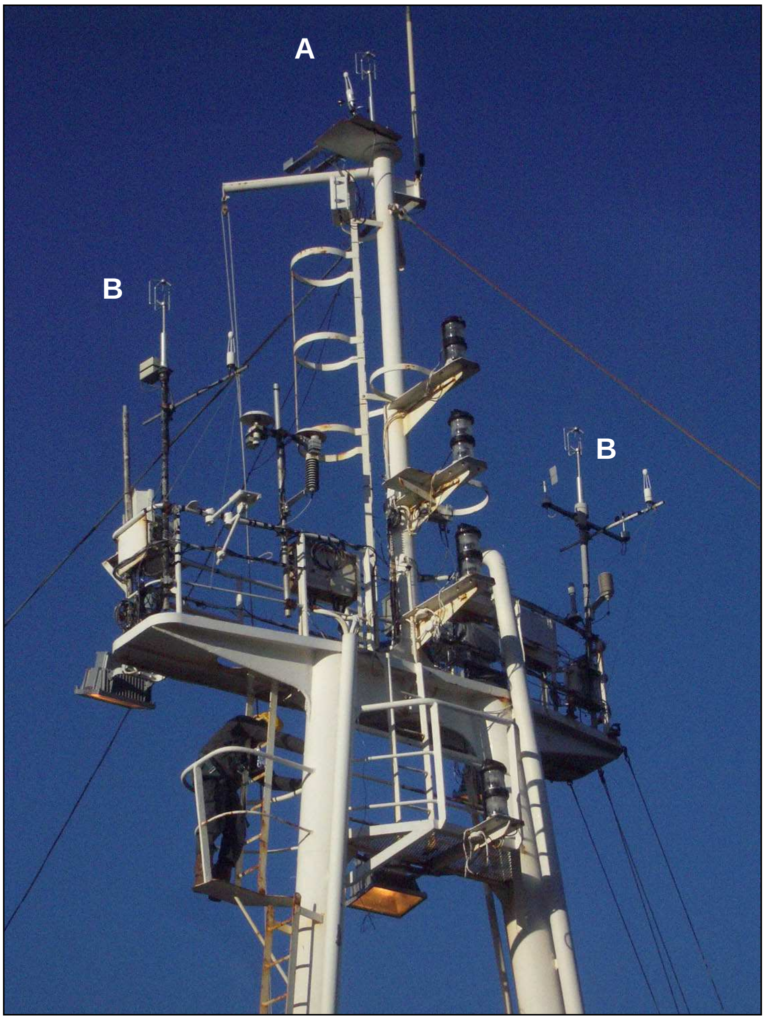

Figure 1. Foremast with Leeds (A) and NOC AutoFlux (B) turbulence systems.

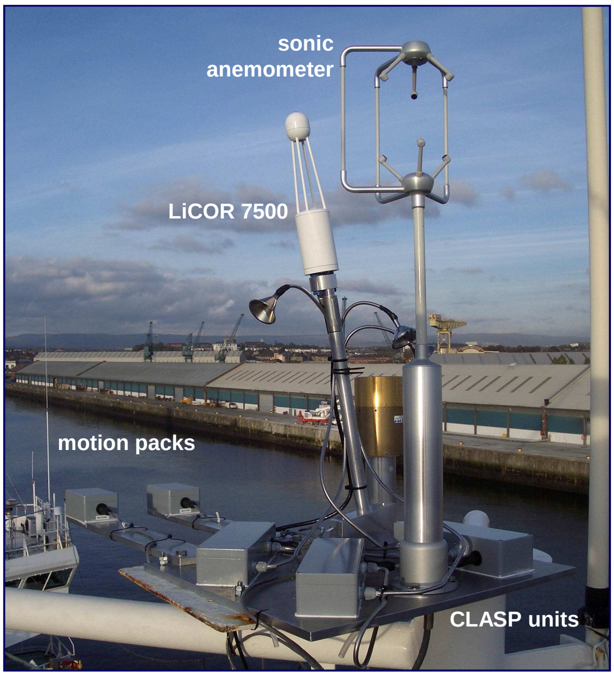

Figure 2. Leeds turbulence instrumentation.

Aerosol Instrumentation

Instruments on monkey island (port side)

Particle Measurement Systems (PMS) Forward Scattering Spectrometer Probe (FSSP)
Aerosol size spectra in range: 0.25 – 23.5 μm (radius) (This instrument failed early during the cruise, and produced no usable data.)

PMS Optical Aerosol Probe (OAP)
Aerosol size spectra in range: 3.55 – 157.5 μm (radius)

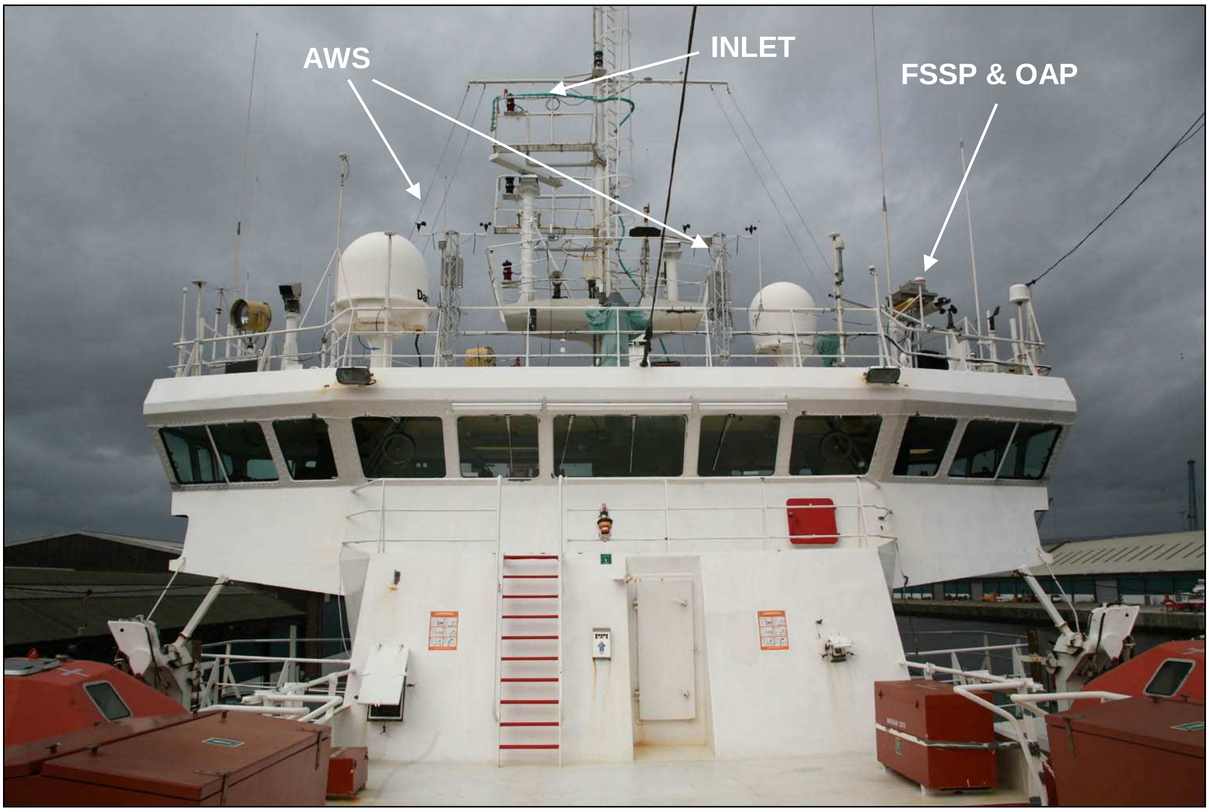

Figure 3. Locations of the FSSP, OAP, and AWS (above). Close up of FSSP, OAP (below).

Instruments in container lab, drawing samples via isokinetic inlets from 2-inch diameter sample line from the mast above the monkey island:

PMS Passive Cavity Aerosol Spectrometer Probe (PCASP)
Aerosol size spectra in range: 0.05 – 3.5 μm (radius).
Grimm dust monitor
Aerosol size spectra in range 0.15 – 10 μm (radius).
Aethalometer
Black carbon loading

VACC – Volatility system

PMS hybrid ASASP-X/PCASP coupled to a software-controlled heated inlet (ambient to 900ºC). Chemical composition and mixing modes of the aerosol are inferred from changes in the spectral shape and number concentration with temperature using the fact that different chemical species become volatile and vaporize at characteristic temperatures.

Particle sizes in range: 0.05 – 1.5 µm (radius).

TSI Aerosol Time of Flight Mass Spectrometer (ATOFMS)

Single particle sizing and chemical composition

Other instrumentation

Automatic Weather Stations (AWS)

Two AWS were sited on port and starboard sides of the monkey island. They are used primarily to provide information on the conditions experienced by the PMS OAP and FSSP on the bridge. Wind speeds and directions are not a good indication of ambient conditions due to flow distortion over the bridge.

Dasibi UV Ozone monitor

Low rate ozone concentration, draws on sample line from monkey island with an intake at approximately the same level as the FLOS instrument on the foremast. This is used as an absolute reference for calibrating the concentrations from FLOS.

This instrument failed early in the cruise.

Buoy Instrumentations

CLASP aerosol probe: 16 channel aerosol size spectra, 0.05-3.5 µm radius, at 10Hz.

Bubble imaging camera. Digitised images of bubbles recorded at 20 frames per second in 5 second bursts, alternating with processing & save to disk. Operates for 2 minutes out of every 5.

Motion pack: 3-axis linear accelerations at 20Hz. Since the buoy is more or less constrained to remain oriented close to the vertical and to move up and down the guide wire, these acceleration measurements are sufficient to determine the buoy's motion over and position on the waves.

Leeds Instrument Operation Periods

	March																					
	21		22		23		24		25		26		27		28		29		30		31	
	am	pm	am	pm	Am	pm	am	pm	am	pm	am	pm	am	pm	am	pm	am	pm	am	pm	am	pm
PCASP	■			■	■	■	■	■	■	■	■	■		■	■	■	■	■	■	■	■	■
OAP	■	■	■	■	■	■	■	■	■	■	■	■	■	■	■	■	■	■	■	■	■	■
FSSP																						
GRIMM	■			■	■	■	■	■	■	■	■	■	■	■	■	■	■	■	■	■	■	■
VOLATILITY	■				■	■	■	■	■	■	■	■	■	■	■	■	■	■	■	■	■	■
ATOFMS														■	■	■	■	■	■	■	■	■
AWS1	■		■	■	■	■	■	■	■	■	■	■	■	■	■	■	■	■	■	■	■	■
AWS2	■		■	■	■	■	■	■	■	■	■	■	■	■	■	■	■	■	■	■	■	■
Aethalometer	■			■	■	■	■	■	■	■	■	■	■	■	■	■	■	■	■	■	■	■
BUOY			■		■		■								■				■		■	
CLASP1		■	■	■	■	■	■	■	■	■	■	■	■	■	■	■	■	■	■	■	■	■
CLASP2		■	■	■	■	■	■	■	■	■	■	■	■	■	■	■	■	■	■	■	■	■
FLOS		■	■	■	■	■	■	■	■	■	■	■	■	■	■	■	■	■	■	■	■	■
Dasibi Ozone		■	■	■	■	■	■	■	■	■												
LICOR		■	■	■	■	■	■	■	■	■	■	■	■	■	■	■	■	■	■	■	■	■
SONIC		■	■	■	■	■	■	■	■	■	■	■	■	■	■	■	■	■	■	■	■	■

	April																					
	1		2		3		4		5		6		7		8		9		10		11	
	am	pm	am	pm	Am	pm	am	pm	am	pm	am	pm	am	pm	am	pm	am	pm	am	pm	am	pm
PCASP	■	■	■	■	■	■	■	■	■	■	■	■	■	■								
OAP	■	■	■	■	■	■	■	■	■	■	■	■	■	■								
FSSP																						
GRIMM	■	■	■	■	■	■	■	■		■	■	■		■								
VOLATILITY	■	■	■		■	■	■	■	■	■	■	■	■	■								
ATOFMS	■	■	■	■	■	■	■	■	■	■	■	■	■	■								
AWS1	■	■	■	■	■	■	■	■	■	■	■	■	■	■								
AWS2	■	■	■	■	■	■	■	■	■	■	■	■	■	■								
Aethalometer	■	■	■	■	■	■	■	■	■	■	■	■	■	■								
BUOY		■					■		■		■		■									
CLASP1	■	■	■	■	■	■	■	■	■	■	■	■	■	■	■	■	■	■				
CLASP2	■	■	■	■	■	■	■	■	■	■	■	■	■	■	■	■	■	■				
FLOS	■	■	■																			
Dasibi Ozone																						
LICOR	■	■	■	■	■	■	■	■	■	■	■	■	■	■	■	■	■	■	■	■	■	
SONIC	■	■	■	■	■	■	■	■	■	■	■	■	■	■	■	■	■	■	■	■	■	

PSO's DAILY LOG

Note, most of the instrumentation operates continuously - during transit as well as when hove to on station – we have relatively few numbered stations, reserving these for buoy deployments only. All times are UTC.

2007/03/21

- Depart Govan 11:15, proceeded directly out to open ocean
- Leeds turbulence and aerosol systems started logging late afternoon.

2007/03/22

- Leeds turbulence systems stopped at 06:50. Electronic compass in motion packs put into calibration mode and ship turned through a 360 degree circle – good compass calibration obtained on both motion packs.
- Turbulence systems restarted at 08:30
- Test deployment of tethered buoy at 09:40 (station D317/001 #1), whitecapping marginal. Buoy recovered at approx 13:00.

2007/03/23

- Arrived on station at 59º47′N 14º31′W at 12:00, hove to for measurements. Wind speed ~16m/s, Hs = 4.3m.
- Intended deployment of tethered buoy postponed due to heavy seas.

2007/03/24

- Measurements continued on station
- Buoy deployed at 09:15 at 59º59.3′N 15º12.2′W (station ID D317/002 #1),
- Buoy recovered at 13:15. Buoy got dragged under just before being recovered – water got into both enclosures and trashed both circuit boards and pumps. Sensing heads survived undamaged – swapped onto spare boards for future deployment.
- CLASP 1 on foremast reporting flow-rate errors. Spectra show much lower counts than CLASP 2. Probably pump failure.

2007/03/25

- Measurements continued on station

2007/03/26

- Measurements continued on station
- Wind dropped during afternoon.

2007/03/27

- Measurements continued through early morning. Wind dropped to ~9.5 m/s, waves to Hs = 2.7m, whitecapping negligible. Forecast indicates winds remain low until at least March 29.
- 08:20 heading SW to reposition at 20W ready for next weather system
- FSSP brought down from monkey island to lab to realign laser.

2007/03/28

- On station at 58º16.5′N 20º06′W
- Buoy deployed at 09:27, station ID D317/003 #1, recovered at 11:20. Data quality poor – particles detected only in smallest 3 channels. Upon subsequent investigation, rubber connecting hose between inlet and sensor head found to be kinked so that larger particles lost to walls. Inlet realigned for subsequent deployments.
- Incinerator burn at 13:00

2007/03/29

- 08:20 headed NW aiming for 60N again.
- Wind from starboard-aft – sampling exhaust fumes for most of day.
- FSSP reinstalled on monkey island at 19:00
- 19:30 - on station at 60N, 22º10′W

2007/03/30

- Buoy deployed at 09:00 at 59º 45′N, 22º 20′W, station ID D317/004 #1

- Buoy recovered at 10:10 on request from bridge due to increasing waves/swell
- FSSP still counting low – alignment still not adequate.
- Incinerator burn at 14:00

2007/03/31

- Buoy deployed at 59º14′N 22º52′W at 09:17, Station ID D317/005 #1
- Buoy recovered at 11:20
- FSSP brought back down to lab.

2007/04/01

- Buoy deployed at 09:05, at 58º56′N 23º27′W, Station ID D317/006 #1
- Whitecaps marginal, and decreased to almost none by time buoy recovered.
- Buoy recovered at 13:30
- 15:45 started steaming south

2007/04/02

- Still steaming south.
- Aerosol concentrations very high – polluted airmass from Europe.
- Winds beam on most of day – no useful turbulence data
- FLOS ozone instrument failed this morning.

2007/04/03

- Still steaming south
- Winds beam on to ship.
- 12:15 – stopped and turned into wind. On station at 50º53′N 23º27′W

2007/04/04

- Remaining on station, wind and whitecaps marginal in morning, increasing slowly.

2007/04/05

- Buoy deployment at 09:10, at 50º19′N 22º46′W, station ID D317/008 #1
- Connector to CLASP on buoy got pulled out at 11:41
- Buoy recovered at 14:10
- 14:15 – started heading for 26 W to get best chance of high winds for late Friday and Saturday.

2007/04/06

- On station at 26ºW at 02:00
- AWS1 temperature sensor failed – replaced with new sensor 09:15
- Incinerator burn at ~10:00
- Buoy deployed at 10:15, at 50º11′N 26º02′W, station ID D317/009 #1
- Buoy recovered at 15:00.
- NOC AutoFlux system crashed sometime today

2007/04/07

- Last day of official science. Turbulence systems and ATOFMS will continue to until Wednesday April 11.
- Buoy deployment at 09:15, at 49º53′N 26º07′W, Station ID D317/010 #1 Bubble camera fault became apparent after deployment, buoy recovered at 09:40, and deployment aborted.
- CLASP 2 on foremast started producing flow-rate errors this morning.
- Started for Lisbon at 17:00
- AutoFlux system rebooted, started logging again at 21:00

2007/04/08

- Transit to Lisbon.
- Data logging still logging on all instruments. No whitecaps.

D317 CRUISE TIMETABLE OF EVENTS

Date	Time (UT)	Event
02/03/07	0900	Author of following report joins vessel in GOVAN, Glasgow
02-07/03/07		Preparing for SEC and Lloyds Surveys
07/03/07		SEC, Radio and Lloyds Survey completed – Deficiencies to tackle
07-12/03/07		Preparing for ISPS, ILO, ISSC surveys.
12/03/07		Above Surveys completed.
14/03/07		Lub Oil loaded (7000 Litres)
15/03/07	0840	Pilot on board
	0912	Clear of Berth – Proceeding out to the Clyde for ENGINE TRIALS
16/03/07	0852	Pilot embarks to bring ship back alongside.
	1108	Vessel back alongside in Govan
	1130	Commence loading BUNKERS (130 Tonne)
	1600	Bunkers loaded.
17/03/07		Divers attending to ADCP
18/03/07		Mobilisation of Cruise D317 begins
20/03/07	1500	Newly joined Scientists familiarised.
21/03/07	0930	Pre-sailing emergency and boat muster for all hands
	1030	Pre sailing checks to all critical equipment
	1051	Pilot on board
	1109	All gone and clear of berth pilotage down Clyde
	1317	Pilot disembarks off Kemplock Point. Navigating down the Firth of Clyde.
	1324	FULL AWAY on passage – Kemplock Pt bore 180˚ T @ 0.48 Miles
	1830	Leaving Firth of Clyde towards the open sea 55 15.0 N 005 35.5 W Course 270˚ T @ full speed
	1912	a/c to 323˚ T 55 15.0 N 005 15.8 W
22/03/07	0000	Position Latitude 55 44.8 N Longitude 006 44.6 W
	0627	a/c to 337˚ T 56 34.8 N 007 59.7 W
	0705	Commenced slow turn – compass checking 56 41.1 N 008 04.6 W
	0742	Compass check complete resume course 56 40.5 N 008 06.7 W
	0943-1307	Tethered Met Buoy deployed **D317 / 01 #1 56 58.2 N 008 17.2 W**
	1312	resumed passage Course 311˚ T @ full speed
23/03/07	0000	Position Latitude 58 15.8 N Longitude 011 04.7 W
	1200	Position Latitude 59 41.5 N Longitude 014 17.3 W
	1254	Hove to on Station **No Designation 59 47.2 N 014 30.5 W**
24/03/07	0000	Still on station – measuring particulates 59 53.2 N 014 55.5 W
	0915-1321	Tethered Met Buoy deployed **D317 / 02 #1 59 59.4 N 015 10.5 W**
	1321	Tethered buoy inboard
	1800	Still on station – measuring particulates 59 57.0 N 015 12.6 W
25/03/07	0000	Still on station – measuring particulates 59 56.6 N 015 17.1 W
	0600	Still on station – measuring particulates 59 54.3 N 015 34.0 W

	1200	Still on station – measuring particulates 59 49.8 N 015 46.9 W
	1800	Still on station – measuring particulates 59 44.0 N 015 58.0 W
26/03/07	0000	Still on station – measuring particulates 59 39.8 N 016 10.3 W
	1200	Still on station – measuring particulates 59 27.3 N 016 28.7 W
	1526	CTD Cable overside with test weight hauling and veering 2 casts of 1300m (total 5200m) 59 29.2 N 016 21.9 W
	1720	CTD cable and test weight inboard
27/03/07	0000	Still on station – measuring particulates 59 38.4 N 016 17.8 W
	0837	Set Course 225˚ T to intercept another weather system further west 59 51.6 N 016 36.3 W
	1200	Position Latitude 59 28.0 N Longitude 017 23.6 W
	1800	Position Latitude 58 43.2 N Longitude 018 51.3 W
	2325	Hove to on station - measuring particulates 58 07.6 N 020 00.4 W
28/03/07	0600	Still on station – measuring particulates 58 15.7 N 020 05.8 W
	0925	Tethered Met Buoy deployed **D317 / 03 #1 58 18.8 N 020 07.4 W**
	1120	Tethered Met Buoy inboard 58 17.7 N 020 08.9 W
	1354-1640	CTD Cable overside with test weight hauling and veering 1 cast of 2350m 58 19.1 N 020 09.1 W
	1800	Still on station – measuring particulates 58 21.0 N 020 08.2 W
29/03/07	0000	Still on station – measuring particulates 58 30.1 N 019 58.6 W Wind strength diminishing
	0600	Still on station – measuring particulates 58 39.8 N 019 42.3 W
	0833	Set Course 315˚ T to intercept better winds further to the north west 58 39.6 N 019 32.5 W
	1330	Hove to to launch RIB – maintenance & test purposes
	1351	RIB Launched and away 59 18.8 N 020 49.5 W
	1420	RIB recovered Set Course 315˚ T 59 18.9 N 020 50.0 W
	2000	Hove to on station - measuring particulates 59 58.7 N 022 10.0 W
30/03/07	0000	Still on station – measuring particulates 59 53.4 N 022 14.4 W
	0600	Still on station – measuring particulates 59 46.6 N 022 13.5 W
	0910	Tethered Met Buoy deployed **D317 / 04 #1 59 45.7 N 022 21.8 W**
	1009	Tethered Met Buoy inboard (too rough) 59 45.7 N 022 22.8 W
	1200	Still on station – measuring particulates 59 44.3 N 022 26.5 W
	1800	Still on station – measuring particulates 59 32.5 N 022 38.7 W
31/03/07	0000	Still on station – measuring particulates 59 24.6 N 022 49.5 W
	0600	Still on station – measuring particulates 59 16.6 N 022 52.2 W
	0917	Tethered Met Buoy deployed **D317 / 05 #1 59 12.9 N 022 52.2 W**
	1118	Tethered Met Buoy inboard 59 11.2 N 022 49.6 W
	1800	Still on station – measuring particulates 59 05.5 N 023 00.3 W
01/04/07	0000	Still on station – measuring particulates 59 01.2 N 023 14.2 W
	0905	Tethered Met Buoy deployed **D317 / 06 #1 58 56.2 N 023 28.0 W**
	1337	Tethered Met Buoy inboard 58 55.0 N 023 26.4 W
	1530-37	XBT deployed 58 54.1 N 023 27.9 W
	1537	Course 180˚ T to intercept better winds further to the South
02/04/07	0000	Position Latitude 57 28.4 N Longitude 023 28.0 W
	1200	Position Latitude 55 17.1 N Longitude 023 28.0 W
03/04/07	0000	Position Latitude 53 07.1 N Longitude 023 28.0 W
	1200	Position Latitude 50 55.3 N Longitude 023 28.0 W
	1218	Hove to to measure particulates 50 53.0 N 023 27.6 W
	1535-1635	Coring Cable veered to 1000 metres for sheave maintenance
	1800	Still on station – measuring particulates 50 52.9 N 023 16.5 W

04/04/07	0000	Still on station – measuring particulates 50 50.1 N 023 05.4 W
	0600	Still on station – measuring particulates 50 43.7 N 022 55.2 W
	0920-1050	Coring Cable veered to 2100 metres for sheave maintenance
	1200	Still on station – measuring particulates 50 38.1 N 022 53.9 W
	1322	Tethered Met Buoy deployed **D317 / 07 #1 50 36.7 N 022 53.1 W**
	1635	Tethered Met Buoy inboard 50 37.6 N 022 51.0 W
	1800	Still on station – measuring particulates 50 35.8 N 022 49.6 W
05/04/07	0000	Still on station – measuring particulates 50 27.9 N 022 48.3 W
	0600	Still on station – measuring particulates 50 21.3 N 022 45.5 W
	0910	Tethered Met Buoy deployed **D317 / 08 #1 50 18.2 N 022 46.7 W**
	1412	Tethered Met Buoy inboard 50 20.0 N 022 43.0 W Set Course 270˚ T
06/04/07	0000	Position Latitude 50 20.0 N Longitude 025 28.0 W
	0150	Hove to to measure particulates 50 19.8 N 025 59.8 W
	1011	Tethered Met Buoy deployed **D317 / 09 #1 50 11.2 N 026 02.7 W**
	1504	Tethered Met Buoy inboard 50 10.9 N 026 01.0 W
	1800	Still on station – measuring particulates 50 08.0 N 026 02.0 W
07/04/07	0000	Still on station – measuring particulates 50 03.4 N 026 08.1 W
	0600	Still on station – measuring particulates 49 56.6 N 026 08.8 W
	0918	Tethered Met Buoy deployed **D317 / 10 #1 49 51.8 N 026 06.5 W**
	0945	Tethered Met Buoy inboard to investigate camera malfunction
50 51.5 N 026 05.6 W		
	1006	Decision made to cancel Tethered Buoy deployment
	1200	Still on station – measuring particulates 270˚ T
	1700	Station work ends Set Course 133˚ T towards Lisbon
49 40.3 N 026 01.0 W **End of Stationary Science.**		

CRUISE MAPS

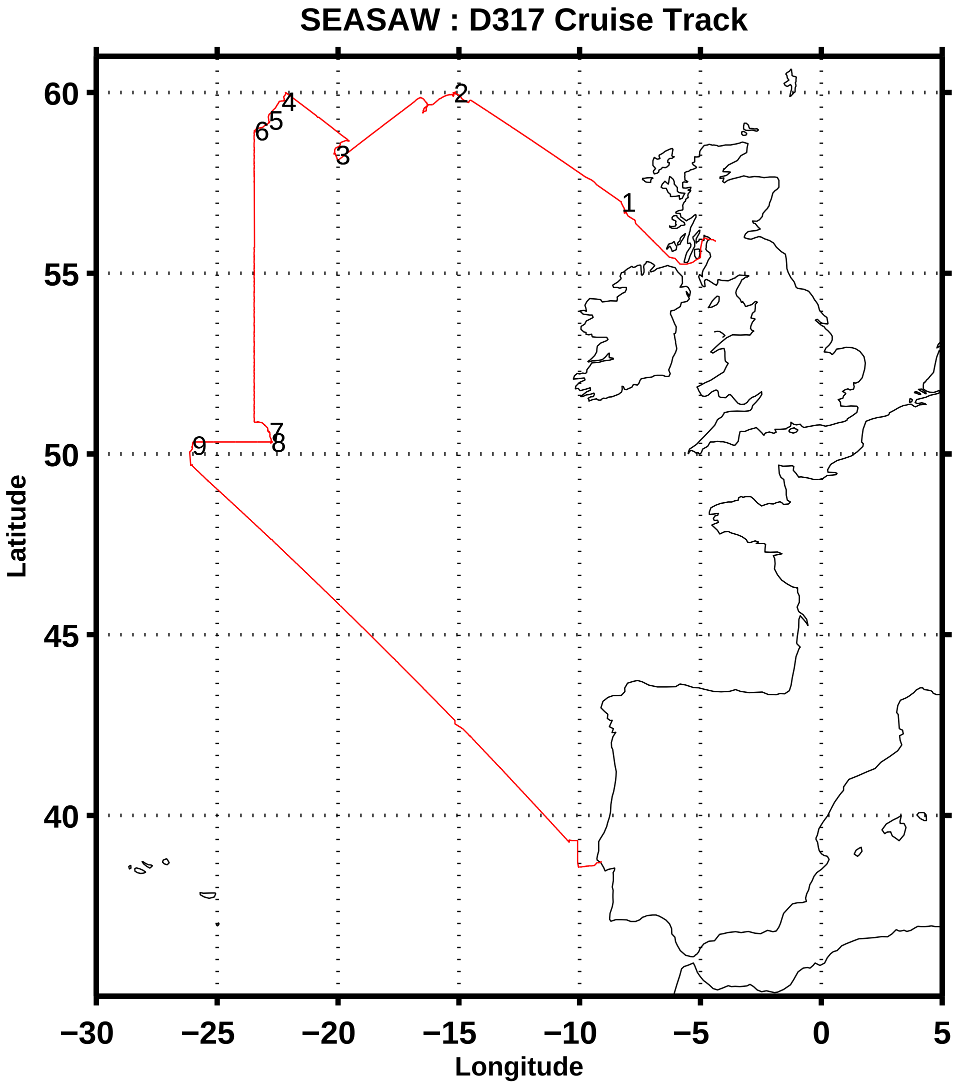

Figure 4. D317 cruise track with buoy deployments indicated.

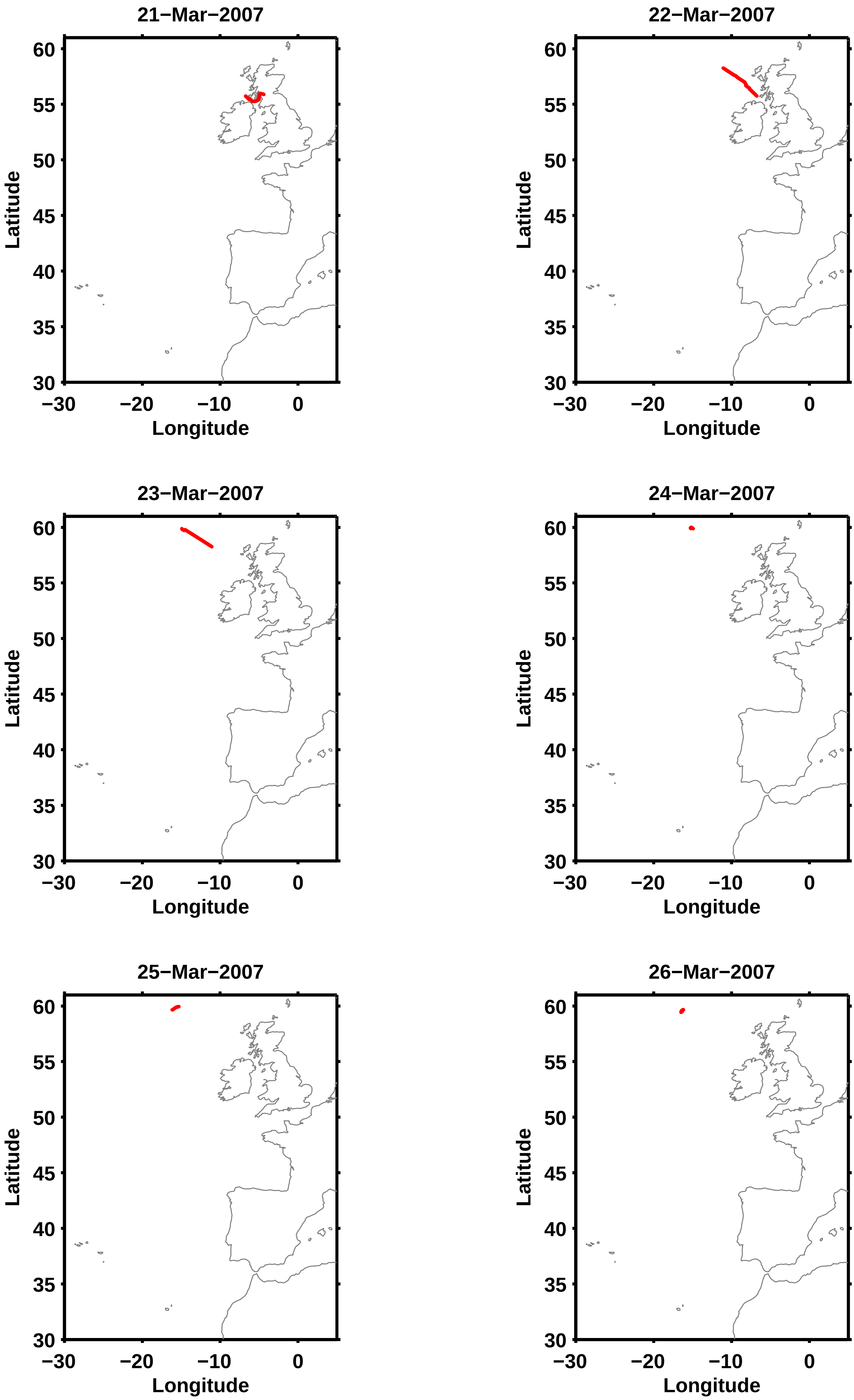
21−Mar−2007
22−Mar−2007
23−Mar−2007
24−Mar−2007
25−Mar−2007
26−Mar−2007
Latitude
Longitude
60
55
50
45
40
35
30
−30
−20
−10
0

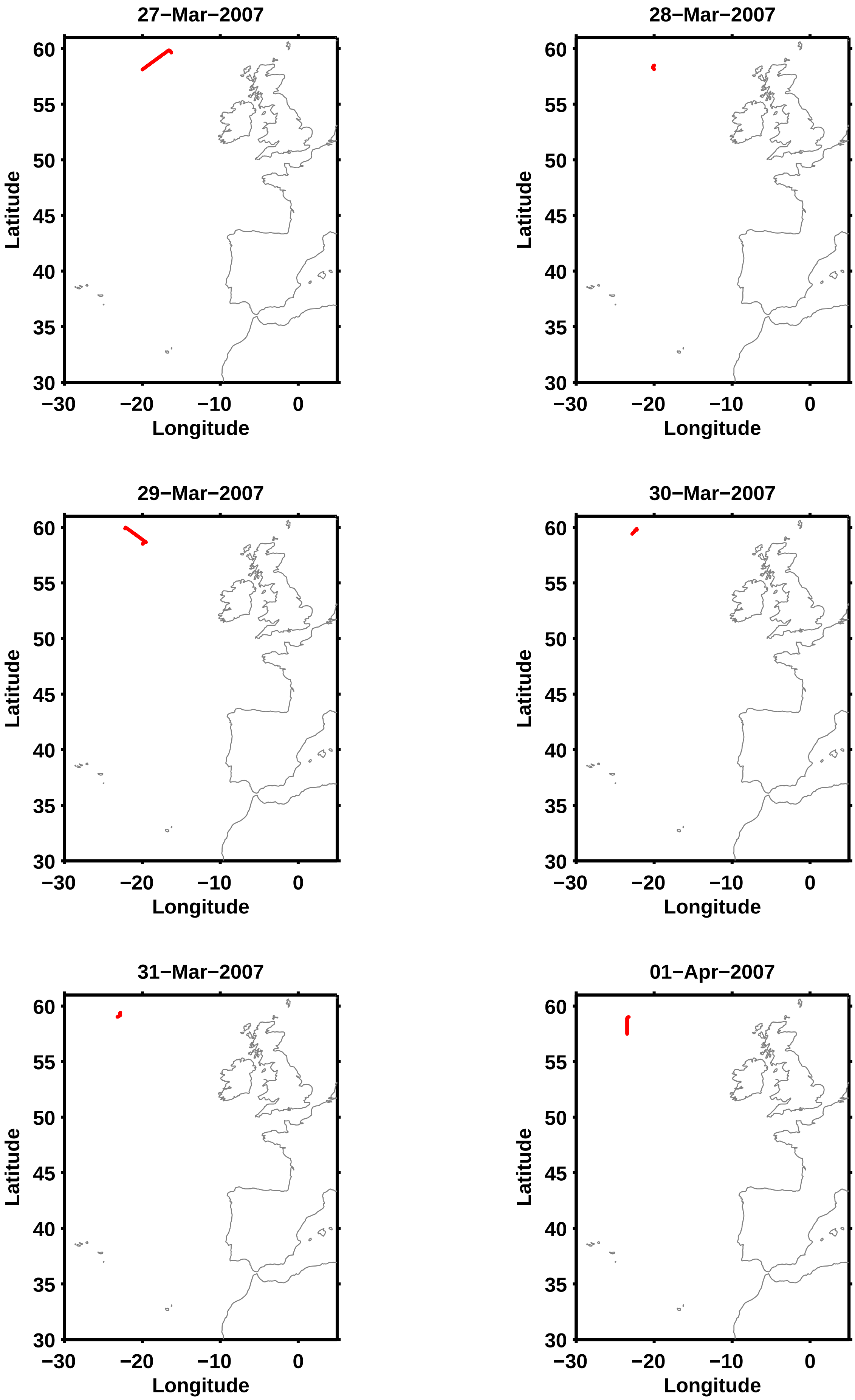
27−Mar−2007
28−Mar−2007
29−Mar−2007
30−Mar−2007
31−Mar−2007
01−Apr−2007
Latitude
Longitude
60
55
50
45
40
35
30
−30
−20
−10
0

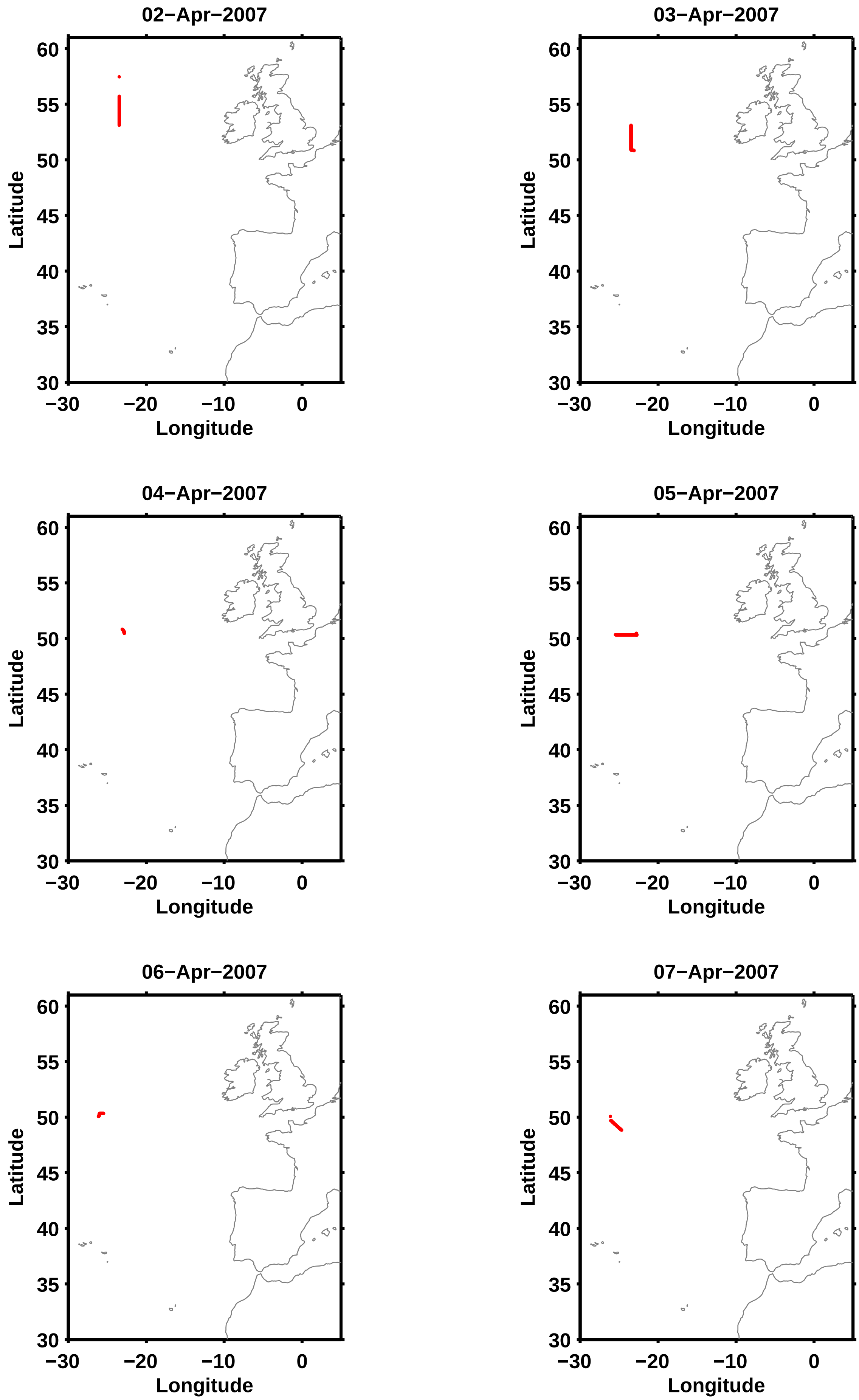
02−Apr−2007
03−Apr−2007
04−Apr−2007
05−Apr−2007
06−Apr−2007
07−Apr−2007
Latitude
Longitude
60
55
50
45
40
35
30
−30
−20
−10
0

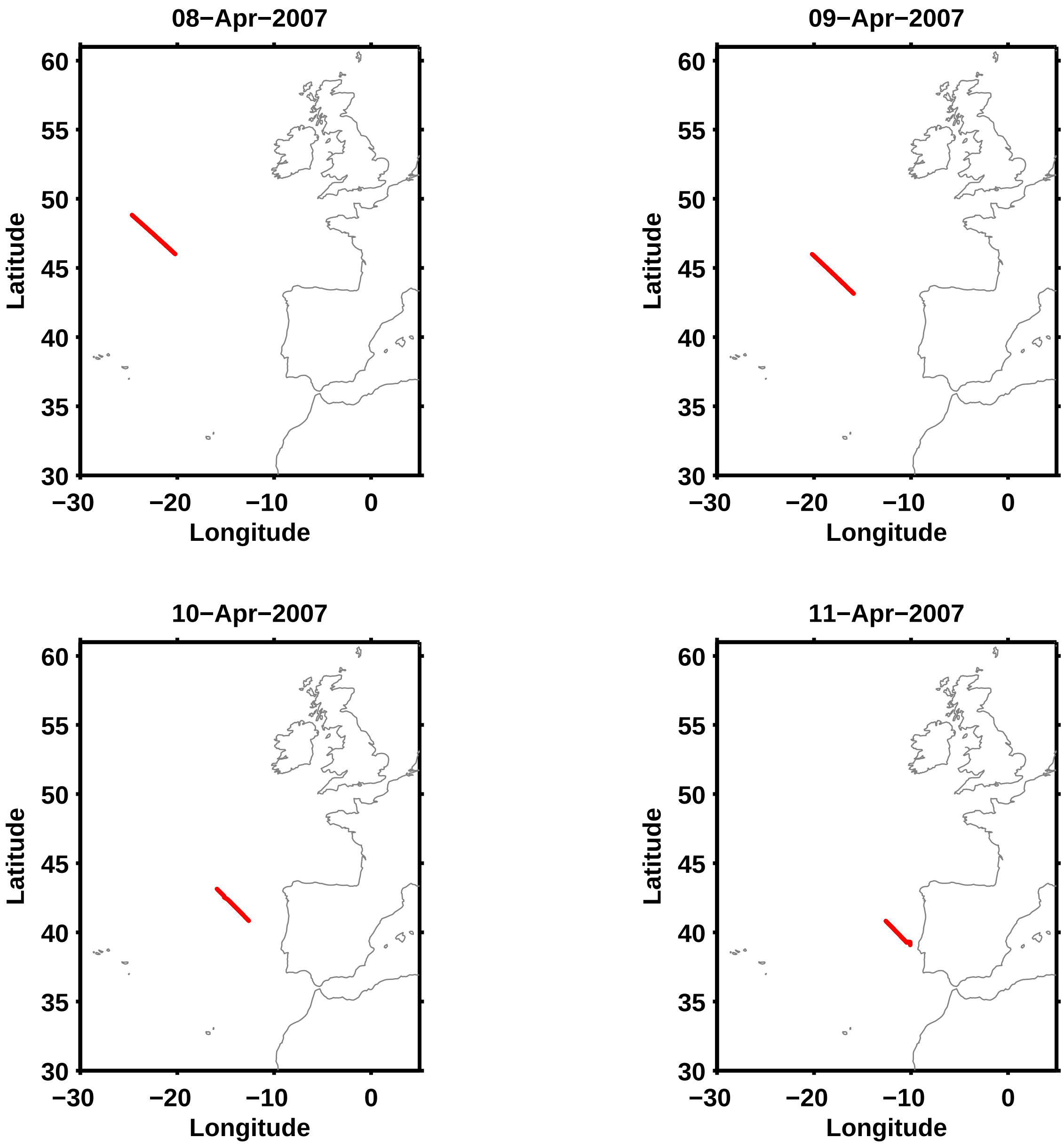
08−Apr−2007
09−Apr−2007
10−Apr−2007
11−Apr−2007
Latitude
Longitude
60
55
50
45
40
35
30
−30
−20
−10
0

LEEDS TURBULENCE MEASUREMENTS

Ian Brooks

The Leeds turbulence instrumentation was installed on the top of the foremast extension with the measurement level at approximately 21.3 m above the waterline. Measurements from the sonic anemometer, LiCOR-7500, CLASP, motion packs, and FLOS were made almost continuously between March 22 and April 11. Data was recorded at 20Hz for a period of 70 minutes, at which point the instruments were stopped and restarted together to minimise the possibility of drift between their individual clocks. The interval between 70-minute logging periods was kept as short as possible, and new files started for each logging period. The whole system was stopped to carry out a data backup first thing each morning and last thing each evening.

Motion Correction

Before calculating turbulent fluxes, the measurements of the turbulent wind components must be corrected for ship motion and attitude. This is undertaken following Edson et al. (1998). Figure 5 shows the power spectral density of the raw and corrected vertical wind component (w) along with that of the vertical velocity of the ship and of the measured waves. The removal of the wave-induced ship motion from the wind is clearly seen.

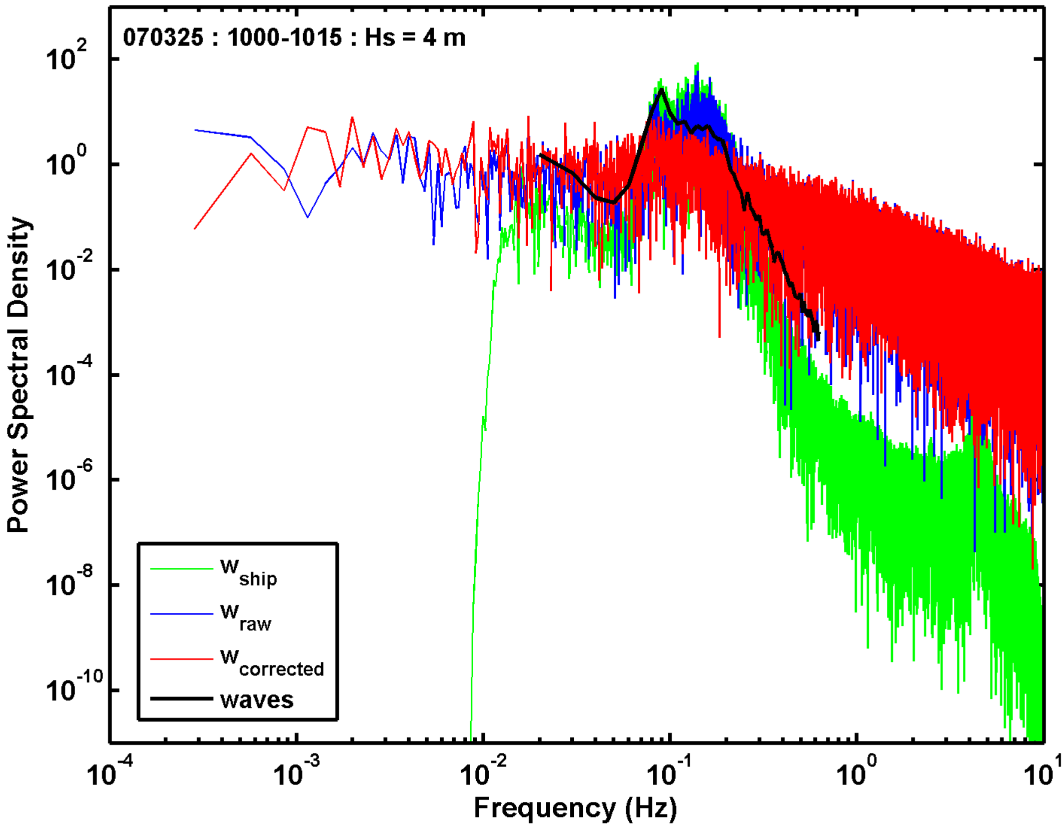

Figure 5. Power spectral density of the raw (blue) and corrected (red) vertical wind components, along with that of the vertical velocity of the ship (green) and the measured waves (black).

Figure 6 shows the result of the motion correction on a short section of the vertical wind time series.

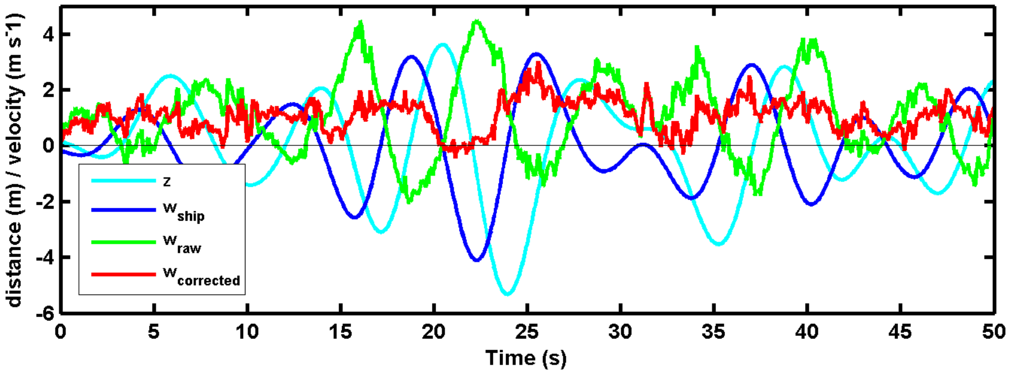

Figure 6. Time series of raw (green) and corrected (red) vertical wind, ship vertical velocity (blue) and ship vertical displacement (z).

After motion correction a total of 1019 15-minute averaging periods were obtained. Fluxes are calculated for every 15-minute period, and flags set according to various quality control criteria – for example, fluxes are only accepted where the mean wind direction is within 30º of the bows (excludes 337 averaging intervals). This allows easy and repeated refinement of the acceptance criteria depending upon the application.

Flux Calculations

The most robust means of estimating a turbulent flux is usually considered to be via the direct eddy correlation technique

$$F_x = \overline{w'x'}$$

where F_x is the kinematic flux, w is the vertical wind, x is the quantity of interest (temperature, moisture content, gas concentration, etc), a prime indicates the perturbation about the mean and the overbar indicates the averaging operator. The average must be taken over a period sufficient to include all scales contributing to the flux (typically >5-10 minutes) but not so long that mesoscale variability or other variations on scales larger than that of turbulent motions contaminates the flux estimate. Here we chose an averaging period of 15 minutes. Eddy correlation is very sensitive to flow distortion around the platform, platform motion, and instrument orientation, requiring careful correction (as above). An alternative approach, insensitive to platform motion, is the inertial dissipation technique (Yelland et al. 1994) – this utilizes the power spectral density of turbulent fluctuations of wind, temperature, etc. within the inertial subrange to estimate the turbulent dissipation and hence derive the scaling parameters u_*, T_*, etc. Although insensitive to platform motion it requires a higher sensor response rate (at least 10Hz). Figure 7 shows a comparison of friction velocities estimated from via inertial dissipation, eddy correlation, and the COARE bulk flux algorithm (v2.6).

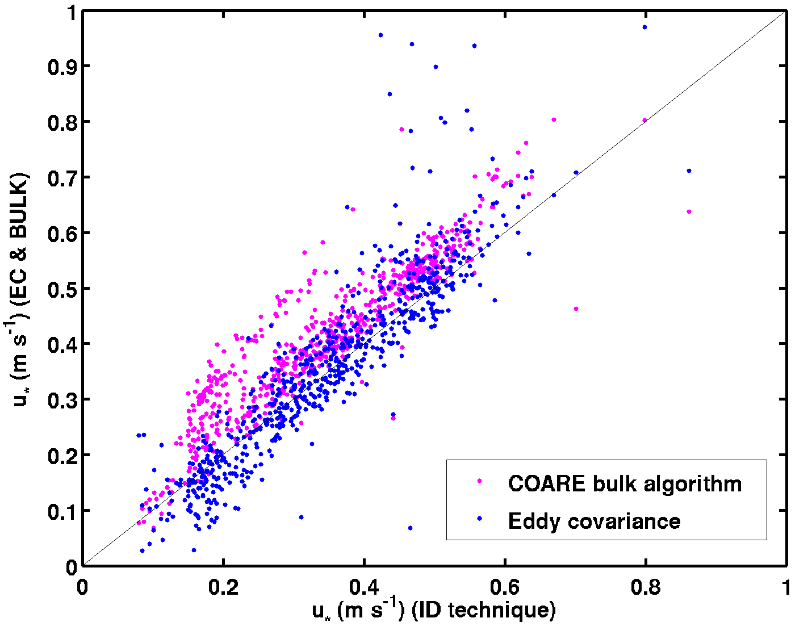

Figure 7. Comparison of 15-minute eddy correlation and bulk flux estimates with those derived from the inertial dissipation technique. The high degree of scatter is typical of turbulence measurements.

Aerosol fluxes

Ian Brooks, Sarah Norris

Almost all sea spray source functions in the literature have been derived via indirect methods. Direct estimates of the sea spray aerosol flux have been attempted in only a handful of cases (Nilsson et al. 2001; Geever et al. 2005; De Leeuw et al. 2007) and these provided only very coarse pseudo size segregation at best. Norris et al. (2007) demonstrated the first fully size segregated aerosol flux measurements via eddy correlation using a new instrument designed and built at Leeds, the Compact Lightweight Aerosol Spectrometer Probe (CLASP)(Hill et al. 2007). A new version of CLASP was deployed for the first time during SEASAW – extending both the size range and number of channels. Measuring just 25 x 8 x 6 cm, CLASP is small enough to be collated with a sonic anemometer (see figure 8), allowing a short inlet without causing significant flow distortion. The operating mode is highly configurable via software; during SEASAW was CLASP output a 16 channel size spectrum at 10Hz for particles between 0.05 and 3.5 μm. Particle fluxes for each channel were calculated over 15 minute averaging periods after screening for wind direction, particle spectra in agreement with background measurements, and checking ogive functions to ensure turbulence was well behaved at the largest scales included in the flux estimate. These are the first fully size segregated eddy correlation aerosol flux measurements to be made over the open ocean.

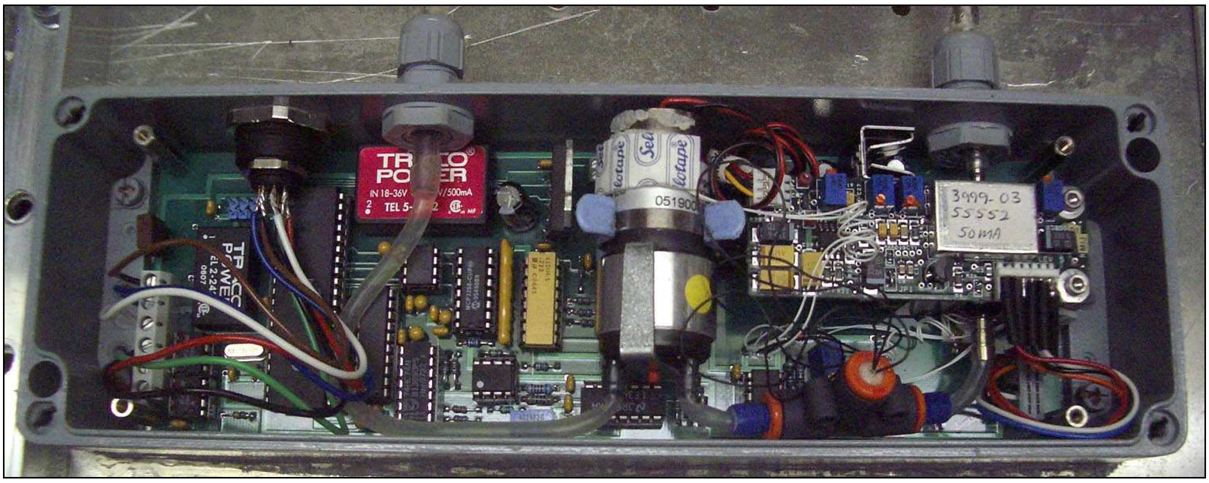

Figure 8. The inside of CLASP. Inlet is at top right of image, outflow to left.

Figure 9 shows ogive functions for aerosol and momentum fluxes for a period of near constant wind speed. The ogive curves are the running integrals of the cospectral energy from high frequency to low – any point on the curve represent the cumulative flux contribution from all high frequencies; the low frequency end point represents the total flux over the averaging period. In well behaved (homogeneous, stationary) turbulence the curves should approach a constant value as seen here for the momentum flux estimates. Significant variability at low frequencies indicates non-stationary conditions.

The ogives for the aerosol flux clearly show much greater variability than those for momentum, both between individual 15-minute averaging periods and at different frequencies for a given curve. The average of all the ogives shown is much better behaved, and demonstrates that the turbulent transport of aerosol takes place over the same scales as that for momentum. We ascribe this high variability to the inherently discrete and spatially variable nature of the surface source of particles: individual whitecaps. This is in contrast to most other scalar fluxes – such as water vapour, temperature, or trace gases – where the surface source is continuous. This means a much higher degree of averaging is required for aerosol fluxes in order to achieve the same degree of statistical certainty in the results.

Figures 10 and 11 show some preliminary estimates of net fluxes plotted against source functions from the literature. These are in reasonable agreement with recent sea spray source functions from the literature. Note that the results presented below are estimates of the net flux and have not yet been corrected for estimates of the deposition flux to derive a source flux. Additional corrections for flow distortion, humidity effects, and particle losses in the inlets may also be required.

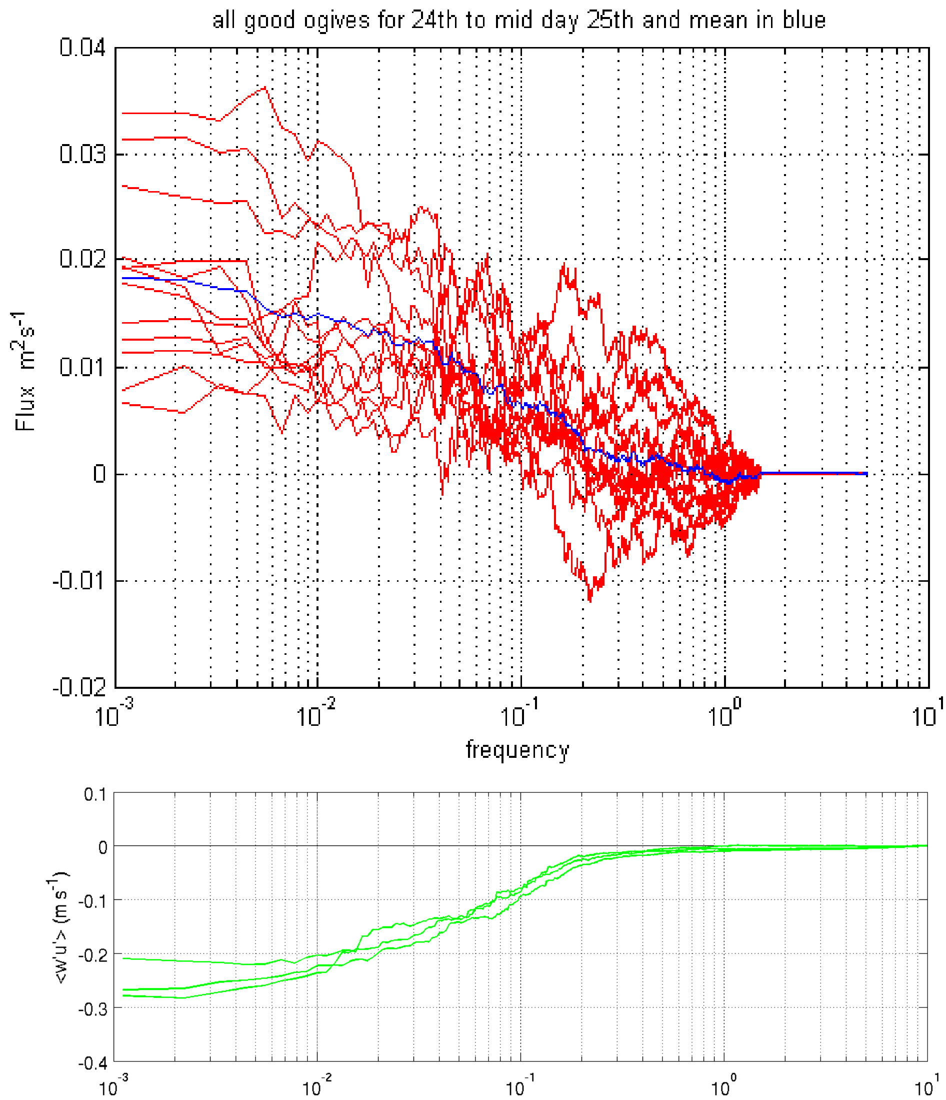

Figure 9. Ogives of aerosol fluxes (upper panel) and momentum flux (lower panel). Red lines are individual 15 minute estimates of the aerosol flux, the blue line is the average of all the ogives shown.

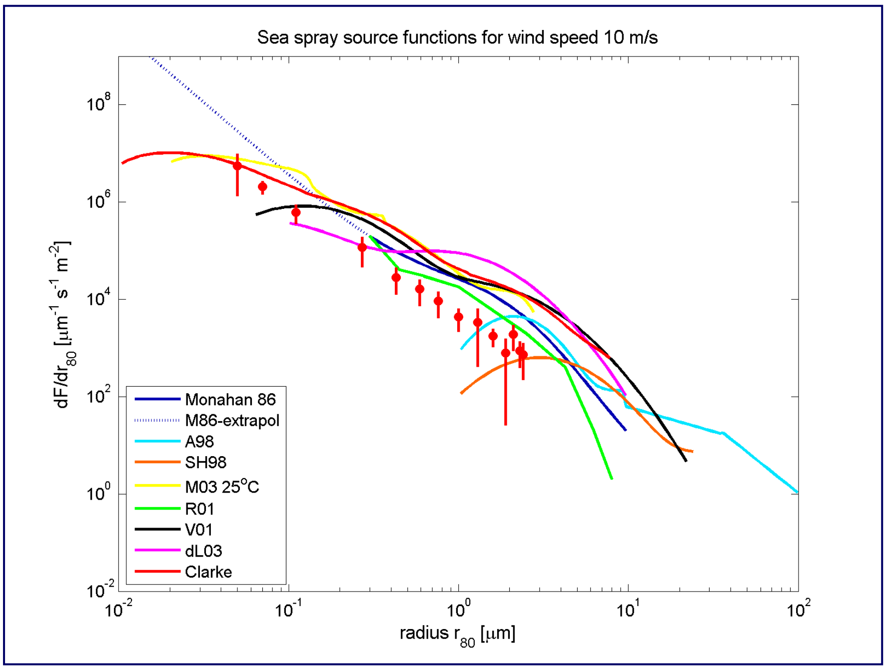

Figure 10. Net aerosol flux estimates and sea spray source functions for U10 = 10 m s^{-1}.

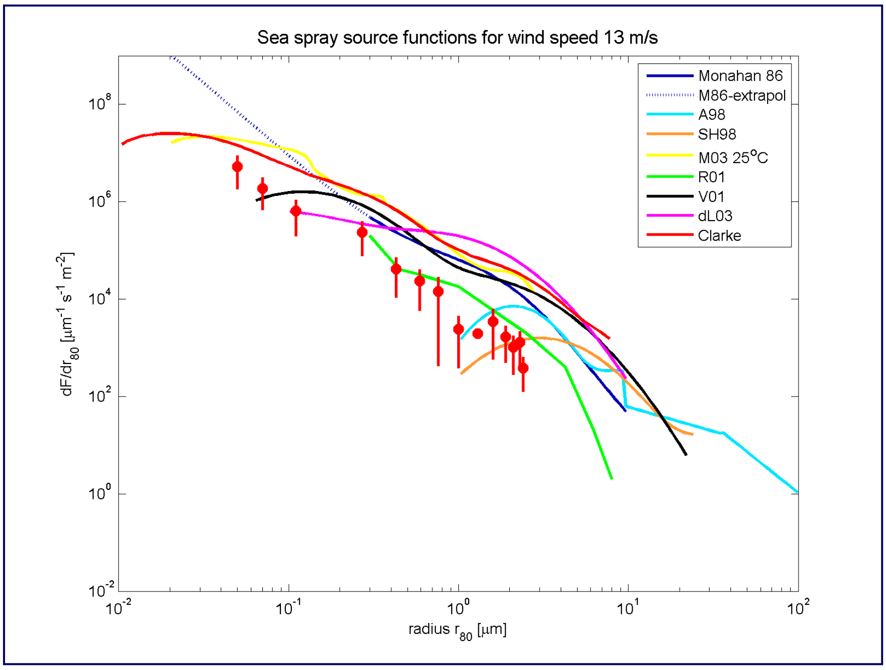

Figure 11. Net aerosol flux estimates and sea spray source functions for U10 = 13 m s^{-1}.

CO_2 fluxes

Ian Brooks, Anthony Bloom

CO_2 concentrations are derived from a LiCOR-7500 open path gas analyzer collocated with the sonic anemometer at the top of the foremast. After preliminary quality control to exclude data segments contaminated by the exhaust of either the *Discovery* or other, passing, vessels initial flux estimates were calculated. In common with previous flux estimates using open path sensors, these were a factor of ~5 larger than predicted by existing parameterizations based on other techniques. Taylor et al. (2007) have recently identified the cause of this problem as being due to a cross-contamination of the CO_2 measurement by water vapour; they have proposed an iterative correction procedure for the flux measurements based on surface layer similarity theory and the assumption that the dimensionless profiles of CO_2 and H_2O are the same. After implementing this correction procedure the CO_2 flux estimates are reduced and brought into general agreement with existing parameterizations. Figure 12 shows the individual estimated transfer velocities before and after correction; Figure 13 shows the transfer velocities averaged into 1 m s^{-1} wind-speed bins. Note that these are preliminary results only – there are a number of known corrections yet to be applied, and further quality control to be undertaken.

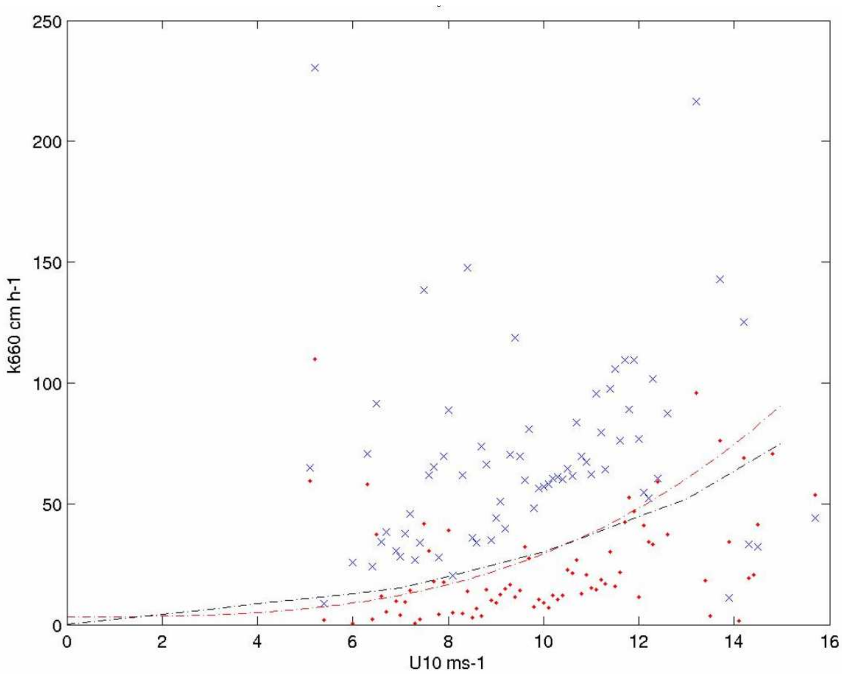

Figure 12. Estimates of CO_2 transfer velocity determined from the uncorrected LICOR data (blue crosses) and after application of Taylor et al.'s (2007) iterative correction (red dots). The dashed lines show the Wanninkhof (1992)(blue) and McGillis et al. (2001)(red) parameterizations.

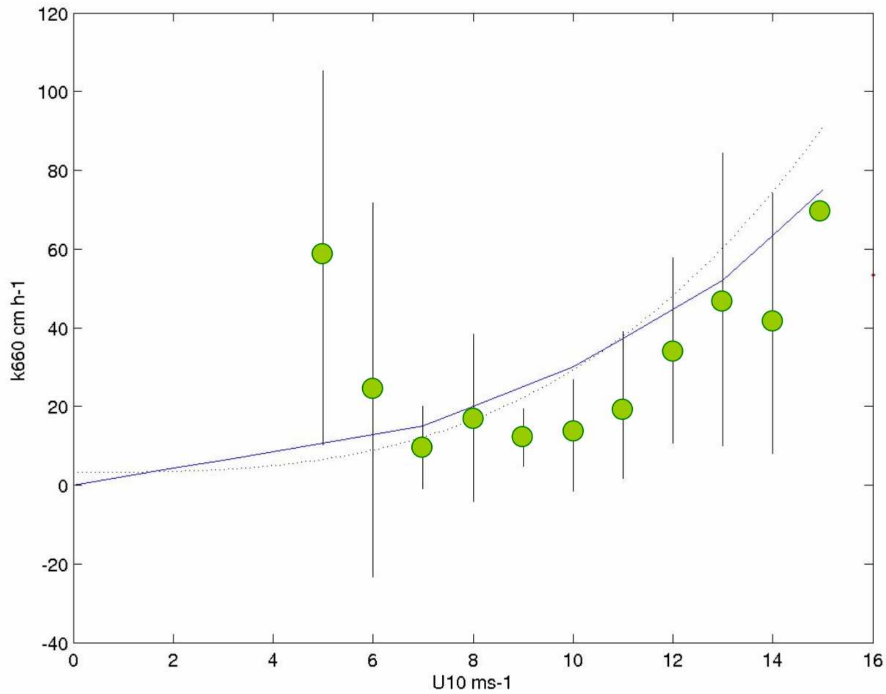

Figure 13. Bin averaged CO_2 transfer velocities, with standard deviations.

Background aerosol

Sarah Norris, Ian Brooks, Barbara Brooks, Justin Lingard

Figure 14 shows the total particle counts from the PMS PCASP and GRIMM dust monitor for the entire cruise, along with the black carbon loading from the Aethelometer.

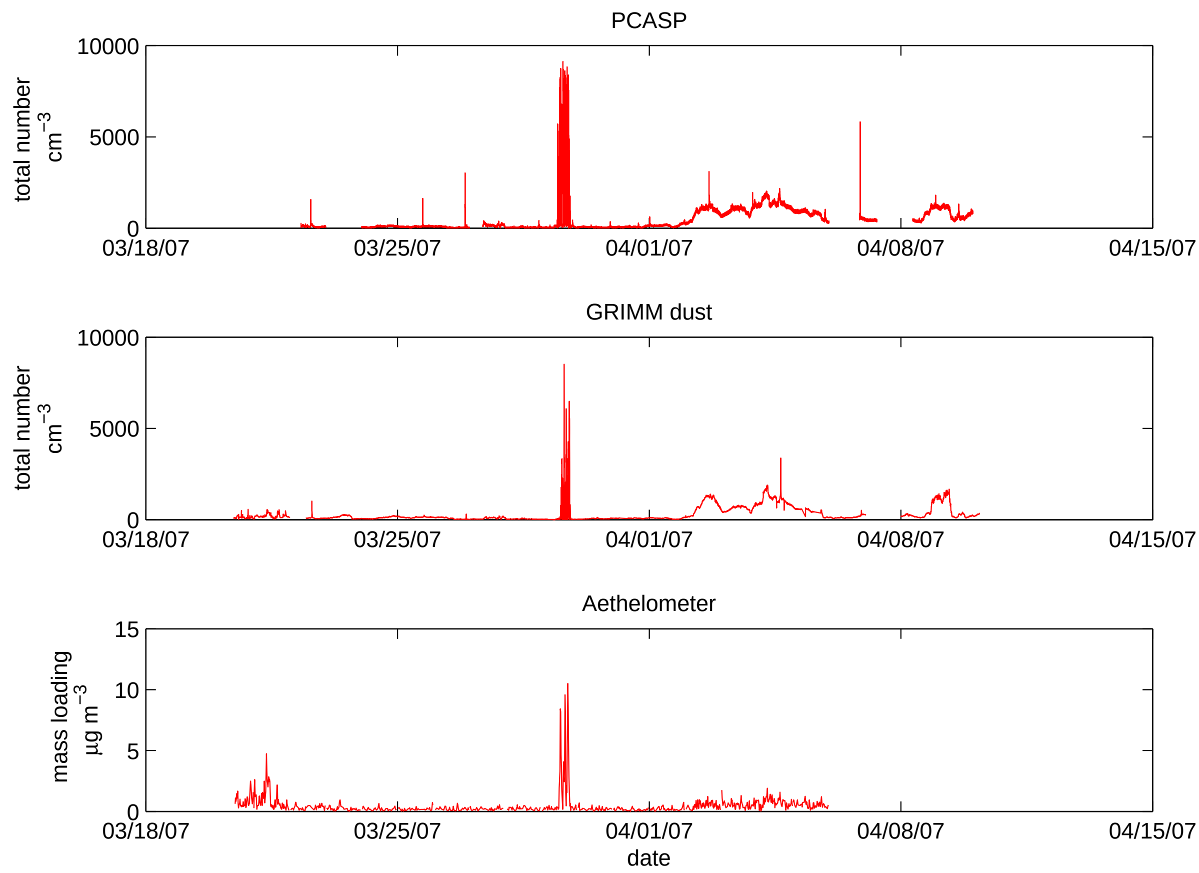

Figure 14. Time series of aerosol total number from PCASP and GRIMM dust monitors, and black carbon mass loading from Aethelometer.

ATOFMS Measurements:

A TSI (Shoreview, MN, USA) 3800 Aerosol Time-Of-Flight Mass Spectrometer (ATOFMS) provided detailed qualitative size-resolved chemical compositional analysis of the sampled marine boundary layer (MBL) aerosol particles. Parallel analysis of both particle radius, within the range of $0.1 \leq R_{va} \leq 0.75$ μm (based on the aerosol's vacuum aerodynamic radius (R_{va})), and composition, was provided via a light-scattering technique coupled with a laser-ablation and dual-ion (bipolar) time-of-flight mass spectrometer. The ATOFMS used was fitted with an aerodynamic focusing lens (TSI AFL-100). Typical particle hit rates varied between 3-13% of the sampled particles. Particle hit rates were dependent on the ambient aerosol number concentration, and tended to be greater for higher particle loadings. Ions produced via laser desorption/ionisation (D/I) produced two mass spectra; one for each polarity of ion, along with the observed particle size distribution. Mass spectra were generated in real-time for each hit (or ‘ablated’) particle and were saved to the on-board data logging computer for subsequent analysis. Regular (daily) calibration of the mass spectrometry region was undertaken throughout the sampling period of the cruise using an atomised solution of NIST SRM 3172a.

Preliminary Results: Sampling was undertaken from 26 March (JD 85) to 8 April (JD 98) 2007. Measurements prior to this period were not obtained due to technical difficulties with the instrument. Within the sampling period, 6,544,570 particles were sampled, of which 420,769 particles were ablated (arithmetic mean hit rate = 6.59%). Processing of the data is on-going. Initial analysis of two contrasting case study days: 31 March (unpolluted) and 5 April (polluted) 2007, demonstrated the outflow of chemically aged particles derived from anthropogenic sources located in continental Europe into the MBL. The ATOFMS data showed that unpolluted marine air masses were dominated by sea salt particles, moreover by the presence of pure sea salt particles. Measurements from the supporting aerosol instrumentation showed that pristine marine air masses were marked by low aerosol particle number concentrations and low black carbon (BC) mass loadings. The ATOFMS measurements demonstrated chlorine displacement in both mixed and aged sea salt particles. This was demonstrative of heterogeneous atmospheric chemistry, namely aerosol-gas interactions with acidic gases namely: HNO_3, NO_x (NO & NO_2), H_2SO_4 and SO_2. The preliminary results suggest that competitive reactions may exist between these acid gases that might influence their uptake onto aerosol particles. Figure 15 shows the daily trend in the ratio of $n(NO_3^-)/n(Cl^-)$[*] containing particles on the unpolluted and polluted days. On the whole, the ratio is greater than unity (represented by the dot-dashed line) during the polluted case study, when NO_x concentrations were expected to be greater due to anthropogenic emissions from mainland sources, and less than unity during the unpolluted case study. The polluted air masses from mainland Europe demonstrated high particle number concentrations and BC mass loadings due to anthropogenic pollution. The ATOFMS measurements demonstrated that this air mass showed enhanced numbers of mixed and aged sea salt particles, as well as carbon-rich particles, composed of typically elemental carbon and primary and secondary organic compounds. The aged nature of the polluted air mass was believed to account for the presence of large numbers of secondary organic aerosol (SOA) particles also detected. Overall, the sampled MBL aerosol particles were extremely heterogeneous in nature and represented complex particle types.

[*] The presence of the NO_3^- ion was inferred the presence of a peak at *m/z* at -52 and Cl^- by a peak at *m/z* at -35 in the derived ATOFMS laser D/I mass spectra.

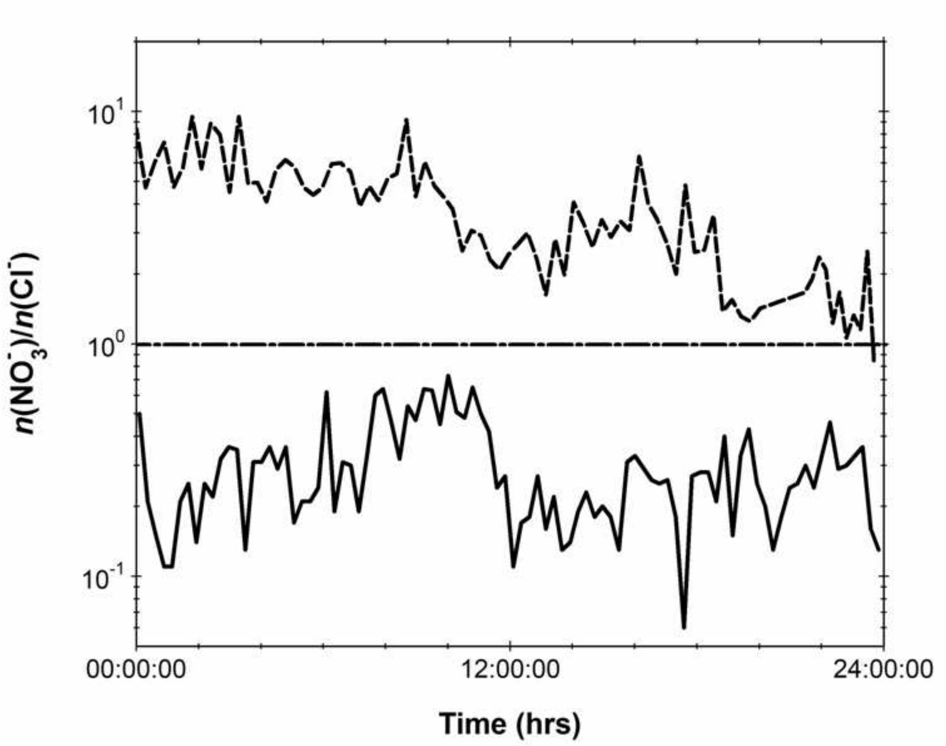

Figure 15. The daily trend in the ratio of $n(NO_3^-)/n(Cl^-)$ containing particles for 31 March (unpolluted) (▬) and 5 April 2007 (polluted) (**- - -**).

AEROSOL VOLATILITY

The VACC (Volatile Aerosol Composition and Counting) instrument incorporates a hybrid PMS ASASP-X/PCASP to size particles in the range 0.05 – 1.5µm (radius) with a software controlled heating system to raise the temperature of the incoming sample to between 40 and 900ºC on a 15 minute cycle. Information on the composition and mixing mode of the aerosol can be inferred from changes in number concentration and spectral shape as different chemical components volatilise at characteristic temperatures. Some examples are given below.

Figure 16 shows the behavior of the bulk aerosol as it is heated. The top plot is number: circles total number of particles counted in the range 0.05 microns < R < 1.5, square counts in the size range 0.05 microns < R < 0.07 microns, up-triangle range 0.07 microns < R < 0.09 microns, douwn-triangle range 0.09 microns < R < 0.2, and pentagrams range 0.2 microns < R < 1.5. For sizes 0.05 to 0.2 the dominant feature is the change in concentration starting at 200 C and ending around 260 C. This is ammonium sulphate transition. Note that for sizes 0.05 to 0.07 there is no variation in number prior to the ammonium sulphate transition, a continual loss of number is however evident in the 0.07 to 0.09 range. This indicates the presence of a long chain hydrocarbon. Volatile organics tend to form a liquid that either encases the core particulate or is an attachment to it (internally mixed) or is a separate droplet population if externally mixed. In either case the volatile component evaporates readily and is lost at temperature below 100. The long chain hydrocarbons tend to lose fragment and are associated with a gradual 'slide ' with temperature. The lower plot shows size/number concentration and from this it can be seen that in the size range 0.2 to 1.5 no ammonium sulphate transition is present but a transition between 600C and 700 is: this being due to sea salt. At all sizes a non volatile (temperature < 800C) residue is present. This is most likely dust – given the back trajectory for this air mass its Saharan dust.

Figure 17 show the number, surface area and volume concentration spectra at temperatures indicated in the legend. It can be seen that between 200C and 300c the only spectral change is in the particles up to 0.2 micron. Further modification occurs between 600C and 700C and this occurs in all sizes but is greatest in sizes >0.1 microns. The spectral behavior between 600 and 700C indicates that sea salt and the non-volatile residue are externally mixed. The spectral behavior between 200 and 300 indicates that the Ammonium sulphate is internally mixed on the other two species but preferentially attached to particles of radii < 0.2.

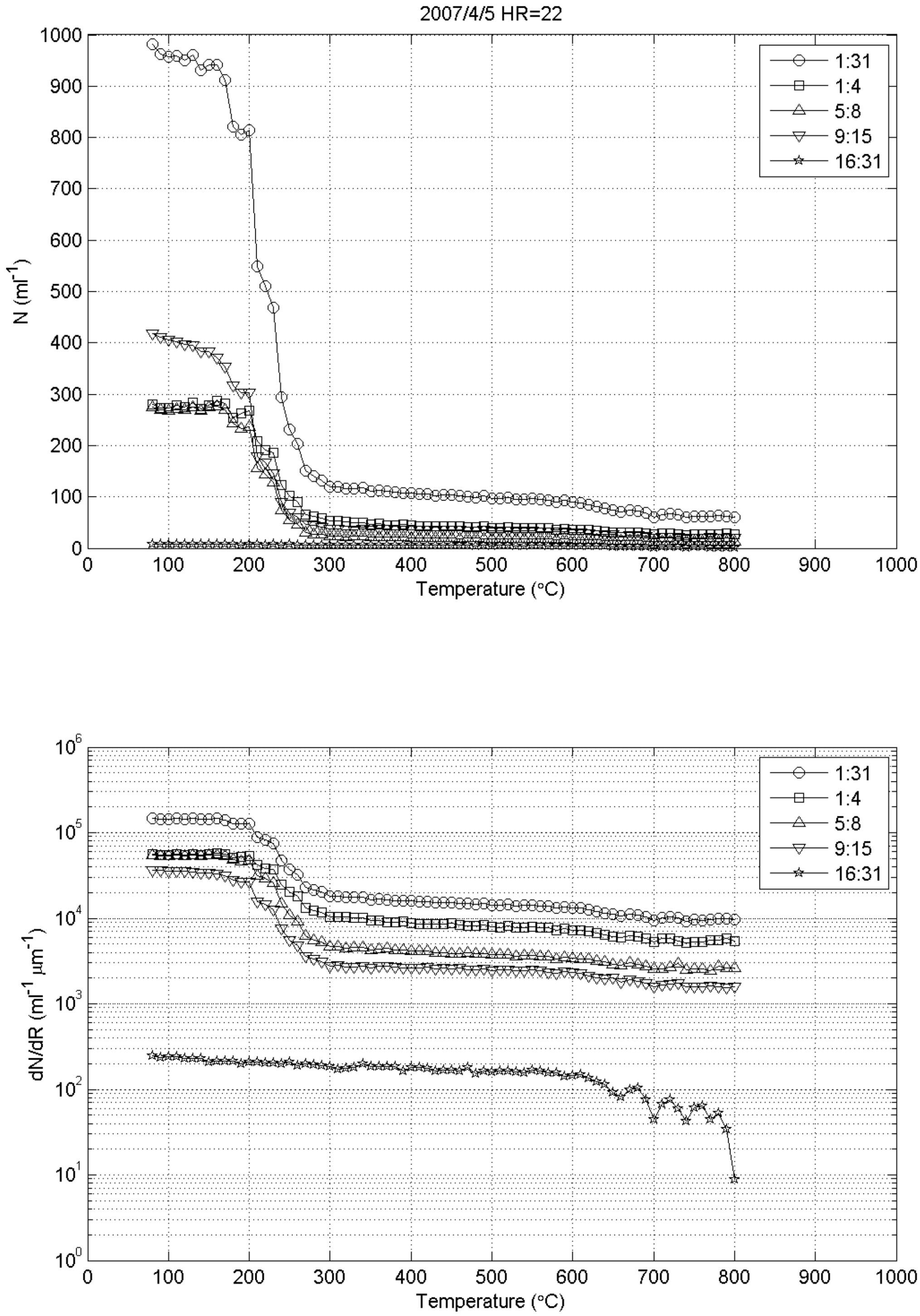

Figure 16: Number and size concentration variation as a function of temperature.

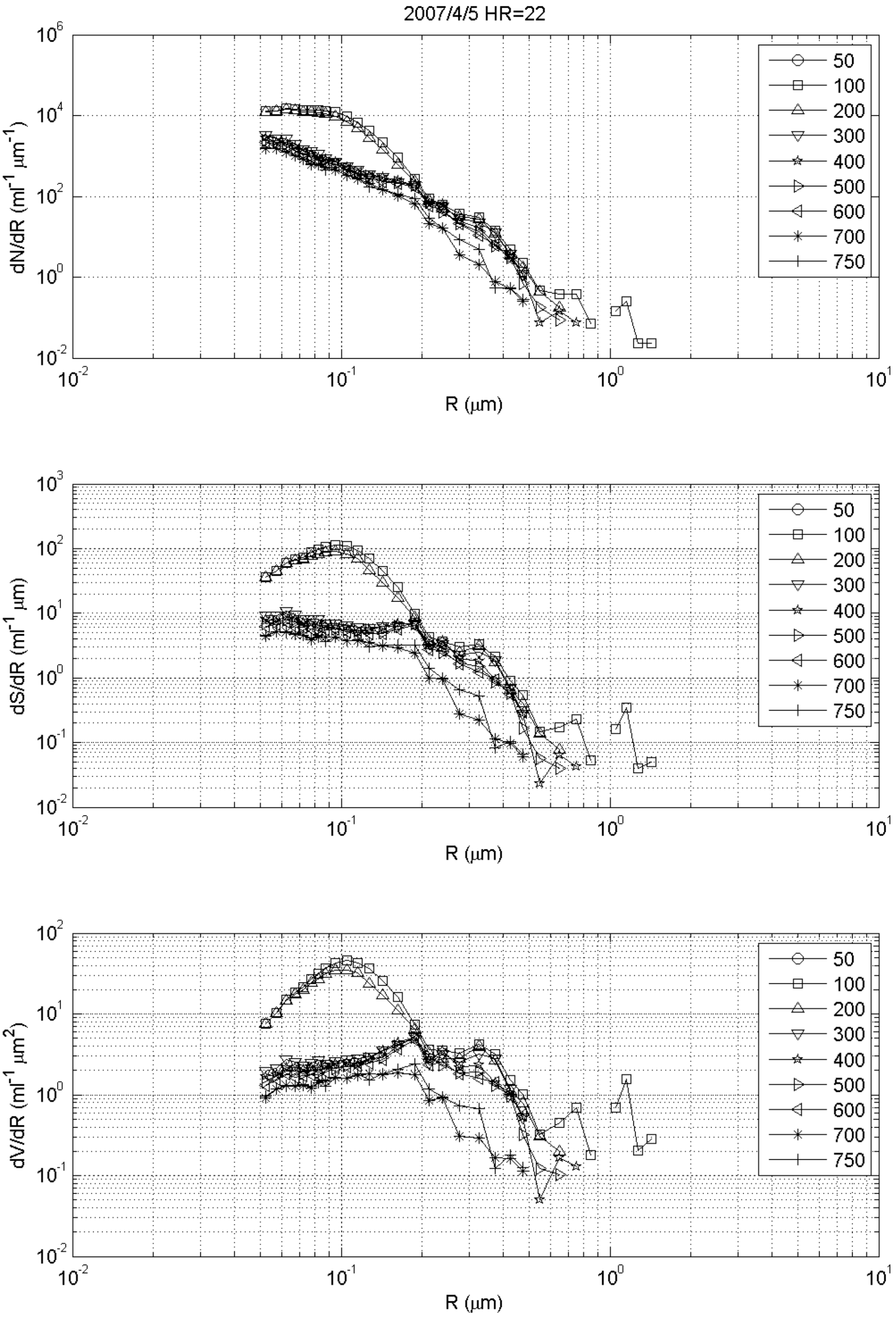

Figure 17. Number , surface area and volume concentration spectra with temperature.

Aerosol Buoy Deployments
Ian Brooks, Sarah Norris

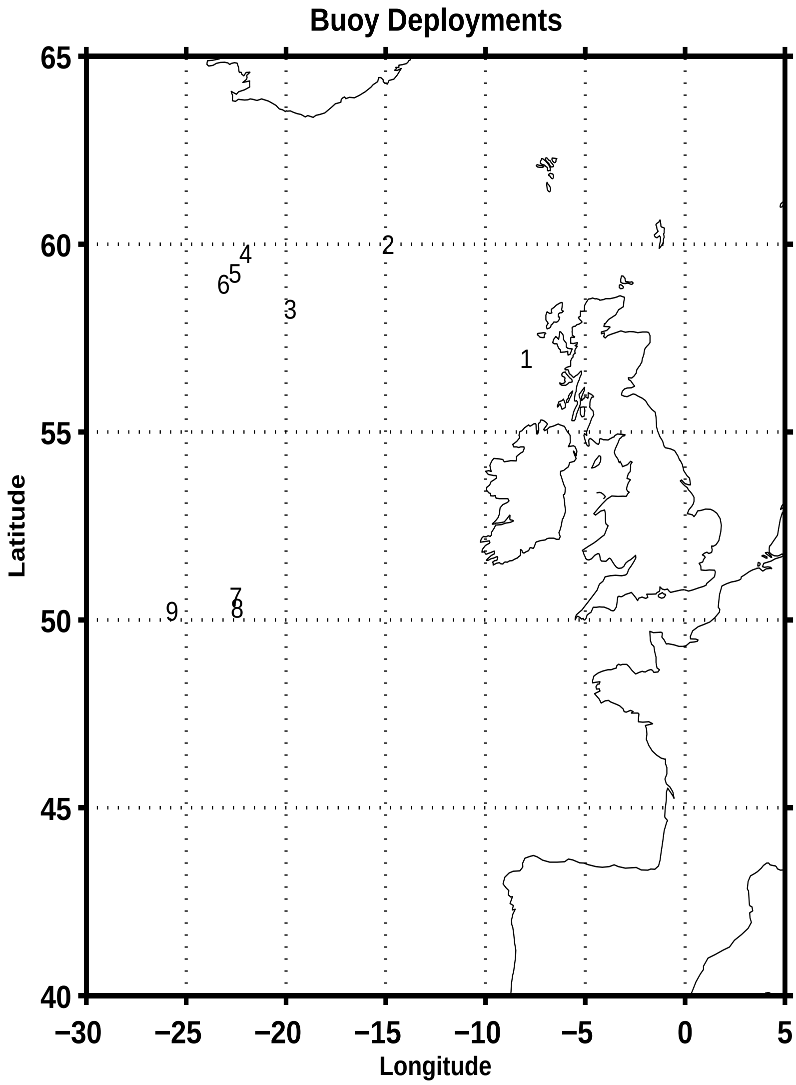

Figure 18. Deployment locations for tethered buoy (numbers refer to station ID D317/n)

Station ID	Date / Time	Comments
D317/001 #1	22/03/2007 09:30 – 13:00	Test deployment. Minimal whitecaps.
D317/002 #1	24/03/2007 09:15 – 13:15	Buoy got dragged under just prior to recovery. Damage to circuit boards on both units. Sensing heads OK after cleaning.
D317/003 #1	28/03/2007 09:27 – 11:20	Buoy deployed with aerosol sensor at 1m only.
D317/004 #1	30/03/2007 09:00 – 10:10	"
D317/005 #1	31/03/2007 09:17 – 11:20	"
D317/006 #1	01/04/2007 09:05 – 13:30	"
D317/007 #1	04/04/2007 13:20 – 16:30	"
D317/008 #1	05/04/2007 09:10 – 11:41	"
D317/009 #1	06/04/2007 10:15 – 15:00	"
D317/010 #1	07/04/2007 09:15 – 09:40	Deployment aborted after failure of bubble imaging camera.

The tethered buoy consisted of a floatation ring with a central gimballed mount attached to a 2-m long steel tube. One or two CLASP aerosol probes are attached to a plate with inlets at approximately 0.5 and 1m above the float. A bubble camera is attached approximately 0.4m below the float. During operation, a cable is passed through the central column, with a lead weight attached to the end. The whole system is then deployed by crane as far off the side of the ship as possible, to keep it out of the region where the water surface is disturbed by the ship. The cable is let out until the weight is about 20m below the surface – the buoy is then kept in position by the cable, but can ride freely up and down it. Power and data cables run back from the buoy to the ship, attached to a rope with floatation aids.

The CLASP unit(s) are identical to those on the foremast, and record aerosol spectra at 10Hz. A motion pack on the buoy, similar to that on the mast, allows the vertical motion and displacement of the buoy to be calculated so that the aerosol spectra can be related to location on the waves.

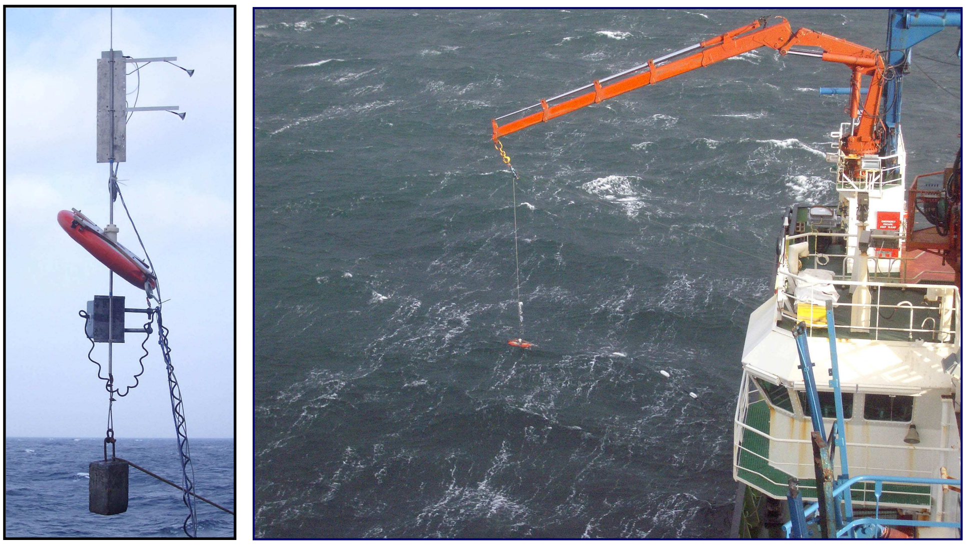

Figure 19. (left) The tethered aerosol/bubble buoy – CLASP units are mounted on the plate above the floatation ring, with their inlets visible on the right; the TNO bubble camera is mounted below the ring. (right) Buoy deployed from ship.

Due to the very high volume of image data, the bubble camera operates in bursts. It captures 100 frames at 20Hz, then pauses while these are processed and written to disk, then repeats the process. This sequence operates for 2 minutes out of every 5. GPS synchronized clocks on the logging systems allow very short periods of bubble and aerosol data to be related to each other; however, since it takes time for the bubbles to reach the surface and burst to form aerosol, and the aerosol sampled by CLASP actually originate some short distance upstream, such highly synchronized comparisons are not particularly useful. Of more interest are average aerosol and bubble populations, along with aerosol flux estimates from the mast, over periods of 15 minutes or longer.

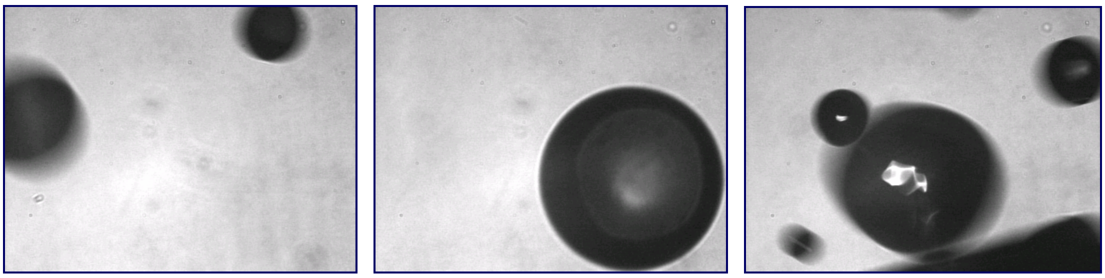

Figure 20. Example bubble images from the TNO bubble camera.

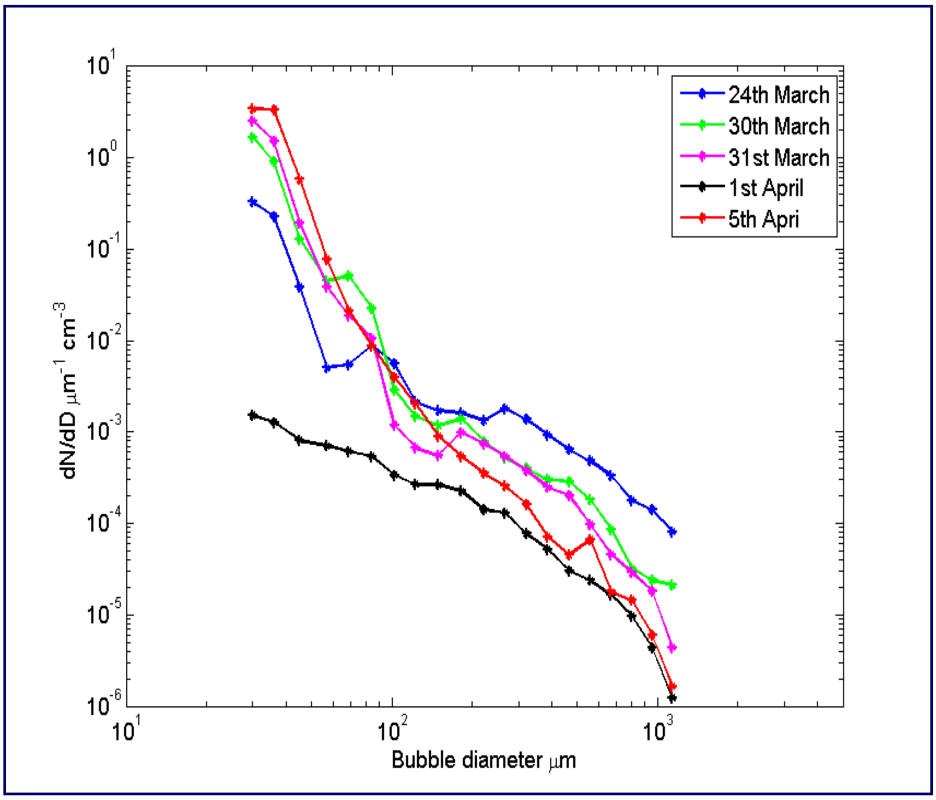

Figure 21. Mean bubble size spectra from five different days

The mean aerosol concentrations are related to mean location on the waves by constructing a joint frequency distribution as a function of vertical displacement and velocity. Figure 22 shows such a distribution for the deviation from mean concentration for 4 different size ranges. It is clearly seen that the concentration is a maximum just forward of the wave crest, just forward of the wave trough.

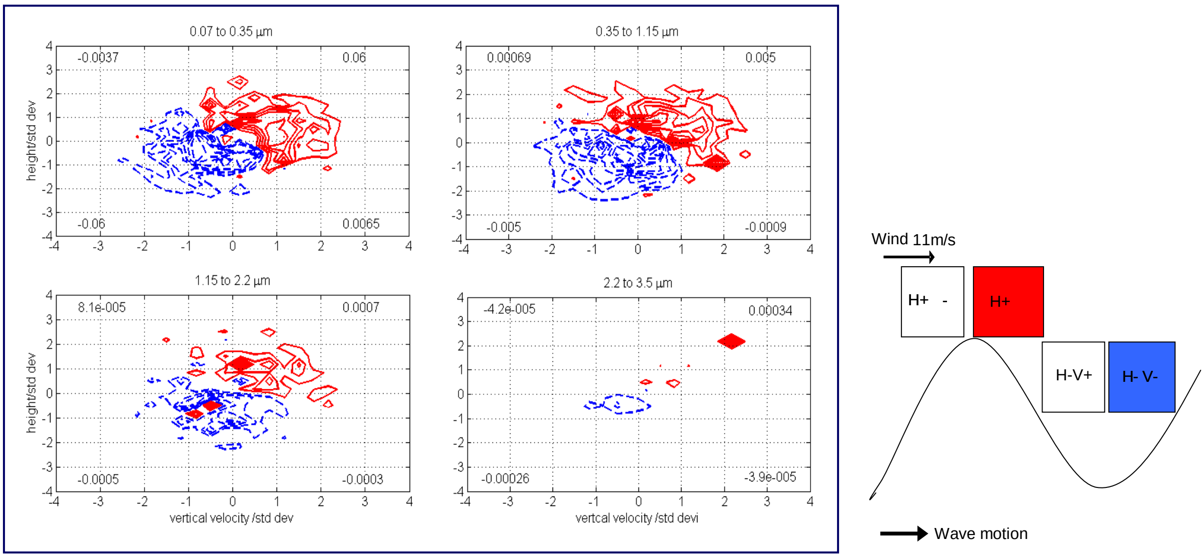

Figure 22. Deviations from the mean aerosol concentration as a function of displacement from mean sea level and vertical velocity (left) and a diagram showing how the regions of higher and lower concentrations of aerosol relate to location on the waves (right).

FLOS – Ozone Measurements
Paul Smith, Jim McQuaid

The Fast and Lightweight Ozone Sensor (FLOS) is a new instrument under development at Leeds. It underwent first field trials during D317. FLOS relies upon the process of chemiluminescence – the emission of light as a result of a chemical reaction. This process is useful for analytical measurements because the reactions take place very quickly and it offers a high degree of sensitivity. There is no requirement for external energy to excite the molecules, so a simple reaction cell and photomultiplier tube (PMT) can be used to count the emitted photons, which are proportional to the concentration of the measured species. Chemiluminescence has been observed with many organic species when oxidised by ozone. These reactions can be utilised to produce a fast-response, sensitive ozone sensor suitable for flux-based measurements.

FLOS uses a wet-chemiluminescent technique based on chromotropic acid, which exhibits chemiluminescence in the presence of ozone. The sensitivity of chromotropic acid to ozone increases by a factor of 100 when combined in an alkaline mixture and exposed to daylight over several days. FLOS utilises this effect by pre-exposing the mixture to UV light to maximise sensitivity, and pumping it onto a translucent wick (Figure 23). This allows heterogeneous-phase chemiluminescent reactions to occur and be detected by a photomultiplier tube (PMT).

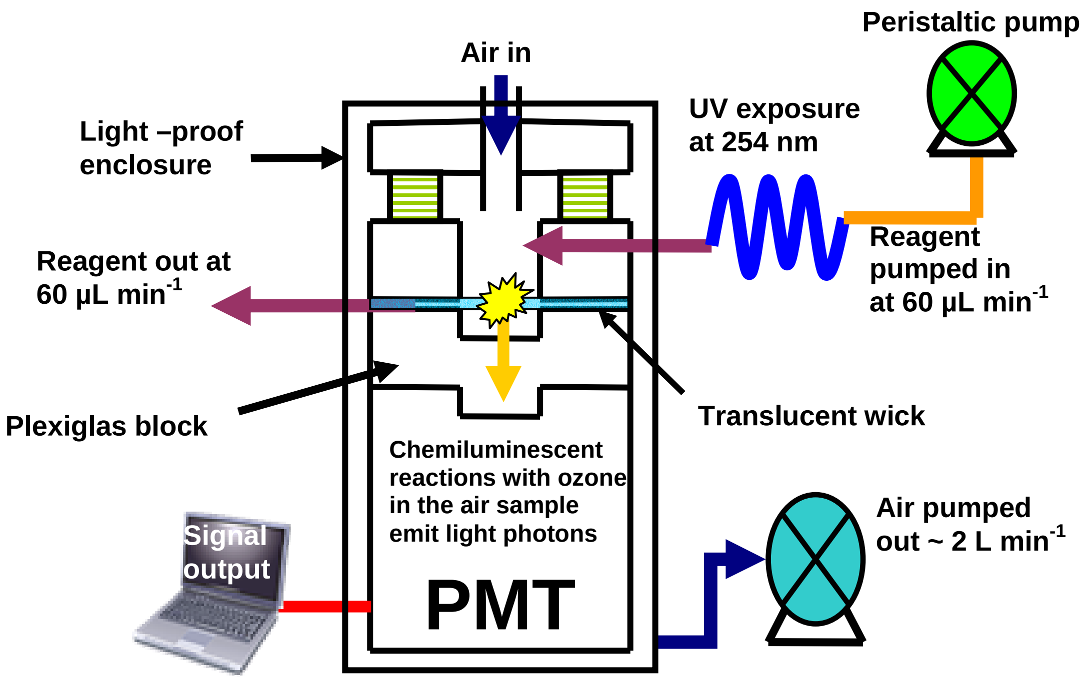

Figure 23. Schematic of FLOS operation.

FLOS was installed on the foremast platform, with a 6.3m long teflon inlet tube run from the top of the mast, next to the LiCOR. It was logged at 20Hz, synchronously with the sonic anemometer. The inlet tube introduces a time lag of 2.3 seconds, corrected during processing. A low rate (0.1Hz) absolute ozone concentration measurement was made by a commercial UV ozone analyser (Dasibi Corp model 1108) located in the container lab, and drawing its sample from above the bridge, at approximately the same level as FLOS. The Dasibi was used to provide a continuous reference against which to calibrate FLOS. Figure 24 shows time series from FLOS and the Dasibi ozone analyzer from early in the cruise. FLOS tracks the Dasibi well; however, after March 23, the Dasibi instrument developed a fault. The mean ozone measurements from FLOS are believed to be reasonable throughout the remainder of the cruise, and its continuous operation has acted as proof of concept for a high-rate autonomous ozone measurement; however, the high frequency noise observed in its output was sufficient to mask any turbulent fluctuations, and no ozone flux estimates were possible. Instrument development continues.

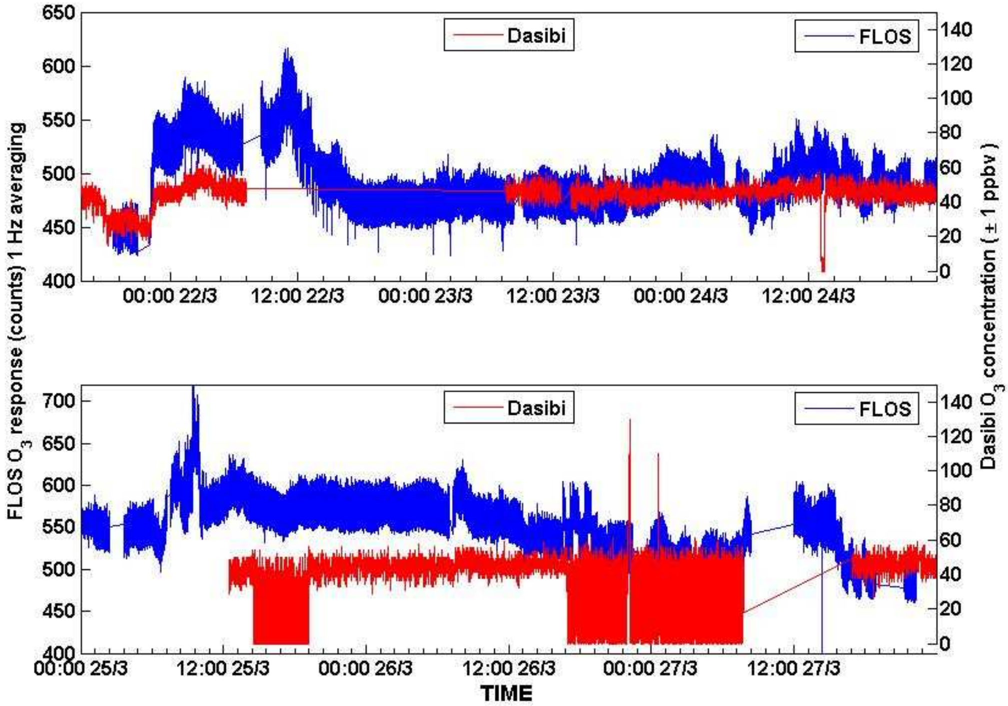

Figure 24. Timeseries from FLOS and the Dasibi ozone analyszer.

1. AutoFlux - the autonomous air-sea interaction system (Ben Moat)

1.1 Introduction

AutoFlux is an autonomous, stand-alone system which obtains direct, near real-time (2 hr) measurements of the air-sea turbulent fluxes of momentum and sensible and latent heat in addition to various mean meteorological parameters. The two main aims of the present deployment were 1) to continuously measure a suite of key meteorological variables (wind speed and direction, air temperature, and humidity, sea surface temperature, short wave radiation and air pressure) and 2) to measure directly the air-sea fluxes of CO_2, sensible heat, latent heat and momentum (by the eddy covariance (EC) and inertial dissipation (ID) methods). The AutoFlux system was mobilised in Govan in February 2004 prior to the start of cruise D277 and left to run autonomously until the beginning of cruise D317. The ID method relies on good sensor response at frequencies up to 10 Hz. The ID method has the advantage that the flux results a) are insensitive to the motion of the ship and b) can be corrected for the effects of the presence of the ship distorting the airflow to the sensors. Momentum and latent heat flux measurements have been successfully made using this method for a number of years. Sensible heat and CO_2 flux measurements are made more difficult by the lack of sensors with the required high frequency response. For these fluxes the EC method provides an alternative. This method requires good sensor response up to only about 2 to 3 Hz, but is a) very sensitive to ship motion and b) the fluxes can not be directly corrected for the effect of air flow distortion. Once EC fluxes are obtained they can be corrected for flow distortion effects by comparison with the corrected ID fluxes where available. Since the scalar fluxes (sensible and latent heat and CO_2) are all affected by flow distortion in the same fashion, only one ID scalar flux is required in order to quantify the effects of flow distortion on EC scalar fluxes.

This report describes the AutoFlux instrumentation (Section 1.2). A brief discussion of the performance of the mean meteorological sensors is given in Section 1.3, where comparisons are made between the ship's instruments with those of AutoFlux where possible. Initial flux results are described in Section 1.4. Appendix A lists significant events such as periods when data logging was stopped, and Appendix B contains figures showing time series of the mean meteorological data. All times refer to GMT.

More information on air-sea fluxes and the AutoFlux project in particular can be found under:

http://www.noc.soton.ac.uk/ooc/CRUISES/AutoFlux/index.php

1.2 Instrumentation

The NOC Surface Processes team instrumented the *Discovery* with a variety of meteorological sensors. The mean meteorological sensors (Table 1.1) measured air temperature and humidity, and wind speed and direction. The surface fluxes of momentum, heat, moisture and CO_2 were obtained using the fast-response instruments in Table 1.2. The MR3 and R3 sonic anemometers provided mean wind speed and direction data in addition to the momentum and sensible heat flux estimates.

To obtain EC fluxes, ship motion data from the MotionPak system was synchronised with those from the other fast response sensors. Navigation data were logged in real time at 1 second intervals, using the ship's data stream. These data are used to convert the relative (measured) wind speed and direction to true wind speed and direction. The ship's mean meteorological '*surfme*t' data were also logged in real time at 2 second intervals to provide access to radiometer and sea surface temperature information. The details of the ship's meteorological instruments are given in Table 1.3.

All data were acquired continuously, using a 55 minute sampling period every hour (the remaining 5 minutes being used for initial data processing), and logged on "ruby", a Sunfire V210 workstation. Processing of all data and calculation of the ID fluxes was performed automatically on "ruby" during the following hour. Program monitoring software monitored all acquisition and processing programs and automatically restarted those that crashed. A time sync program was used to keep the workstation time synchronised with the GPS time stamp contained in the navigation data. Both “ruby” and all the AutoFlux sensors were powered via a UPS.

All of the instruments were mounted on the ship’s foremast (Figure 26.1) in order to obtain the best exposure. The psychrometers, radiation sensors and the fast response sensors were located on the foremast platform. The heights of the centre of the sensor volume of the instruments above the foremast platform were: R3 sonic anemometer, 2.75 m; MR3 sonic anemometer 2.7 m; psychrometers 1.77 m; both Licor H_2O / CO_2 sensors 1.85 m.

1.3 Mean meteorological parameters

1.3.1 Air temperature and humidity

Two wet and dry-bulb psychrometes were installed on the foremast and performed well during the cruise.

A comparison of one minute averaged data from the two psychrometers showed that the starboard psychrometer wet bulb read high by 0.06ºC (standard deviation of 0.06ºC). The difference between the dry bulb temperatures was only 0.02ºC (standard deviation of 0.06ºC). A comparison between the Autoflux Vaisala air temperature sensor and the psychrometer data showed the former read high by 0.08 ºC (standard deviation 0.12ºC). The air temperature measured by the ship’s Vaisala read high by 0.2ºC (standard deviation 0.16ºC) when compared to the Psychrometer measurement. In addition, the difference between the two Vaisala temperature measurements was only 0.12ºC (standard deviation of 0.1ºC). Therefore, the Vaisala air temperature sensors performed well during the cruise and are close to the accuracy of the psychrometer air temperature measurements.

The relative humidity’s calculated by the psychrometers were compared to the measurements made using the AutoFlux and surfmet Vaisala sensors. The ship’s Vaisala was the most accurate of the two and read high by 1.3% (standard deviation of 1.8%). The AutoFlux Vaisala humidity read low by 2.7% (standard deviation of 1.5%). A comparison of the humidity measured by the two Vaisala sensors showed the autoflux Vaisala read low by 4.0% (standard deviation of 1.5%).

1.3.2 Wind speed and direction.

There were three anemometers mounted on the foremast platform (Figure 26.1). On the port side were the ship’s propeller anemometer and the fast response MR3 sonic anemometer. An R3 sonic anemometer was located on the starboard side. Both sonic anemometers measured all three components of wind speed and both are calibrated on a regular basis. The starboard R3 anemometer was the best exposed and will be used as the reference instrument in the following comparison. The measured wind speeds (uncorrected for ship speed) from the MR3 sonic anemometer was compared to those from the starboard R3 in Figure 26.2, which shows the wind speed ratio (measured / R3 measured) against relative wind direction. A wind blowing directly on to the bows is at a relative wind direction of 180 degrees. For a bow-on wind, the MR3 sonic read high by about 1 %. Accurate flow distortion corrections have yet to be determined for the precise anemometer locations, but previous work (Yelland et al. 2002) has shown that the bias at the MR3 sonic anemometer sites should be between -1 and +2%. Figure 26.2 also clearly shows the effects for flow distortion are, as expected, very sensitive to the relative wind direction. The large dips in the speed ratios at 90 and 270 degrees are due to the R3 and MR3 anemometers being in the wake of the foremast extension for winds from the port and starboard beams respectively. Figure 26.3 shows the difference in relative wind direction as measured by each anemometer compared to that from the R3. For bow-on winds the R3 and MR3 agree to with 4 degrees, but the ship’s anemometer appears to be misaligned by 12 degrees.

1.3.3 TIR and PAR sensors.

The ship carried two total irradiance (TIR) sensors, one (Ptir) on the port side of the foremast platform and the other (Stir) on the starboard. These measure downwelling radiation in the wavelength ranges given in Table 1.3. A comparison of the TIR short-wave sensors showed that both sensors were in good agreement. The average of the daily mean differences in the measured short-wave values were about 1 W/m^2 (standard deviation 8.9 W/m^2). In addition to the TIR sensors the ship carried two PAR sensors measure down-welling radiation in the wavelength ranges given in Table 1.3. The starboard PAR sensor read high by 4 W/m^2 (standard deviation of 3.9 W/m^2). It was not possible to check the serial numbers on the PAR sensors during the cruise so it is not clear if the correct calibrations were applied.

1.3.4 Sea surface temperature.

Sea surface temperature (SST) data from the thermosalinograph (TSG) was logged on the AutoFlux system as part of the "surfmet" data stream.

1.3.5 Ship borne wave recorder (SBWR).

The SBWR was switched on prior to the ship leaving Govan. Raw and processed data were logged internally and half hourly wave statistics were transferred automatically to the AutoFlux system via a serial link. The raw data was backed up periodically during the cruise. The time on the SBWR PC used for logging the data was set to GMT in Govan on Jday 078 prior to sailing. At the end of the cruise the PC's internal clock was 125 seconds slow when compared to GMT. The largest wave measured during the cruise was 9.2 m peak to trough on Jday 83.

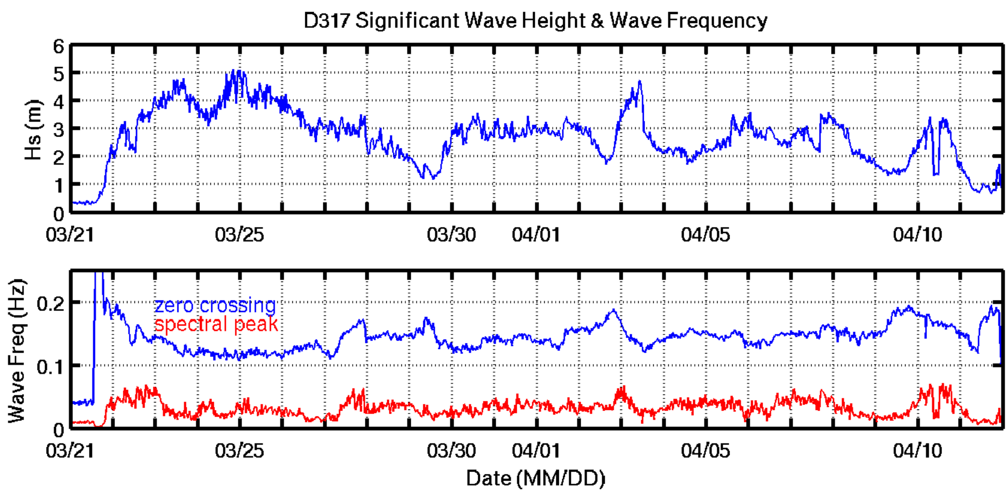

Figure 25. Significant wave height (top) and frequency (bottom) of wave zero crossing (blue) and spectral peak (red)

1.4 Initial flux results.

1.4.1 Inertial dissipation (ID) flux measurements.

The **ID momentum flux** data obtained from the starboard R3 and MR3 sonic anemometers are shown in Figure 26.4 where the drag (transfer) coefficient is shown against the true wind speed corrected to a height of 10 m and neutral atmospheric stability. The drag coefficient is defined as (10^3 * momentum flux / wind speed^2). The mean drag to wind speed relationship from previous cruises (Yelland et al., 1998) is also shown. Only data obtained for winds blowing within ±15 degrees of bow-on were used.

MR3 momentum flux measurements between Jday 87 to 92 were anomalously high in comparison to the R3 measurements and were removed, but after day 92 the instrument seemed to recover. The sensible and latent heat flux measurements obtained from the MR3 sonic temperature data and port Licor H_2O data were also removed between Jday 87 to 92. The reason for bad data will be investigated post cruise.
Figure 26.5 shows the **ID latent heat flux** obtained from the Licors H_2O data. It can be seen that both sensors are producing similar results that agree well with the flux estimated from a bulk formula (Smith, 1988).
Figure 26.6 shows the **ID sensible heat flux** obtained from the R3 and MR3 sonic anemometer temperature data. In this case the measured fluxes are biased high. This is due to high frequency noise contaminating the temperature spectra at all frequencies above about 2 Hz.

1.4.2 Eddy correlation (EC) flux measurements.

The EC fluxes will be worked up post-cruise.

1.5 Summary

The following cruise objectives were met:

a) Meteorological measurements of the key variables were made (wind speed and direction, air temperature and humidity, short wave radiation, sea surface temperature and air pressure).

b) Direct measurements of the air-sea fluxes of sensible heat, latent heat and momentum fluxes were made using the inertial dissipation method. Direct covariance fluxes of these fluxes and the CO2 flux will be produced post cruise.

Acknowledgements

The AutoFlux system was developed under MAST project MAS3-CT97-0108 (AutoFlux Group, 1996) and developed with support from the NOCS Technology Innovation Fund. Participation in cruise D317 was supported by the UK-SOLAS project SEASAW (NERC grant number NE/C001869/1).

Tables

Sensor	Channel, variable name	Address	Serial No.	Calibration Y = C0 + C1*X + C2*X^2 + C3 *X^3	Sensor position	Parameter (accuracy)
Psychrometer 1	1 pdp1	$ARD	IO2002 DRY	C0 -10.247060 C1 3.7734160E-2 C2 2.8237530E-6 C3 -3.5458960E-10	Starboard side of foremast platform	Wet and dry bulb air temperatures and humidity (0.05°C)
Psychrometer 1	2 pwp1	$BRD	IO2002 WET	C0 -10.056430 C1 3.797148E-2 C2 2.6190290E-6 C3 -2.8233060E-10		
Psychrometer 2	3 pds2	$CRD	IO1029 DRY	C0 -1.2649590 C1 3.9241630E-2 C2 9.7851460E-7 C3 3.9947880E-10	starboard side of foremast platform	Wet and dry bulb air temperatures and humidity (0.05°C)
Psychrometer 2	4 pws2	$DRD	IO1029 WET	C0 -1.3705870 C1 4.0089460E-2 C2 9.4633060E-8 C3 7.9263180E-10		
Vaisala	5	$ERD	X4120001 Hum	C0 0.0 C1 0.1	port side of foremast platform	0 – 100 %
Vaisala	6	$FRD	X4120001 Air	C0 -39.65 C1 0.1		-20-60 degC

Table 1.1. The mean meteorological sensors. From left to right the columns show; sensor type, channel number, rhopoint address, serial number of instrument, calibration applied, position on ship and the parameter measured.

Sensor	Program	Location	Data Rate (Hz)	derived flux / parameter
Gill R3 Research Ultrasonic Anemometer serial no. 227	Gillr3mpd	starboard side of foremast platform	20 Hz	momentum and sensible heat
Licor-7500 CO_2 / H_2O sensor serial no. 75H0614	licor3		20 Hz	latent heat and CO_2
Gill MR3 Research Ultrasonic Anemometer serial no. (n/a)	gillmr3d	port side of foremast platform	20 / 100 Hz	momentum and sensible heat
Licor-7500 CO_2 / H_2O sensor serial no. 75H0825	licor3b		20 Hz	latent heat and CO_2
MotionPak ship motion sensor serial no. 0682	via gillr3mpd	starboard side of foremast platform	20 Hz	EC motion correction

Table 1.2. The fast response sensors.

Name	Sensor	Type	Serial no.	Sensitivity	Cal
STIR	Kipp & Zonen CM6B (335 – 2200 nm)	Pyranometer	047462	11.84 µV/W/m2	8.4459459E4
PTIR	Kipp & Zonen CM6B (335 – 2200 nm)	Pyranometer	047463	10.63µV/W/m 2	9.4073377E4
PPAR	Skye energy sensor (400-700nm)	PAR	28558 (not checked)	1mV/100W/m 2	n/a
SPAR	Skye energy sensor (400-700nm)	PAR	28557 (not checked)	1mV/100W/m 2	n/a
Pressur e	Vaisala PTB100A	Barometric	S361 0008 **(U1420016?)**	800–1060 mbar	n/a
wind speed	Vaisala WAA151	Anemometer	P50421	0.4-75 m/s	n/a
Wind Dir	Vaisala WAV151	Wind Vane	S21208	-360 deg	n/a
Air temp	Vaisala HMP44L	Temp	U 185 0012	-20-60 degC	slope 1.0891 offset: 1.78
			A2150009	-20-60 degC	slope: 1.044 offset: -0.6
humidit y	Vaisala HMP44L	Humidity	U 185 0012	0-100%	slope 1.0891 offset: 1.78
			A2150009	0-100%	slope: 1.044 offset: -0.6

Table 1.3. The ship's meteorological sensors.

Difference from psychrometers	Mean difference	Standard deviation
AutoFlux Vaisala humidity	2.7 % low	1.5 %
Ship's Vaisala humidity	1.3 % high	1.8 %
AutoFlux Vaisala temperature	0.08 °C high	0.12 °C
Ship's Vaisala temperature	0.2 °C high	0.16 °C

Difference from AutoFlux Vaisala	Mean difference	Standard deviation
Ship's Vaisala humidity	4% low	1.5 %
Ship's Vaisala temperature	0.12 °C high	0.1 °C

Table 1.4. Mean differences between the temperature and humidity sensors.

1.8 Figures

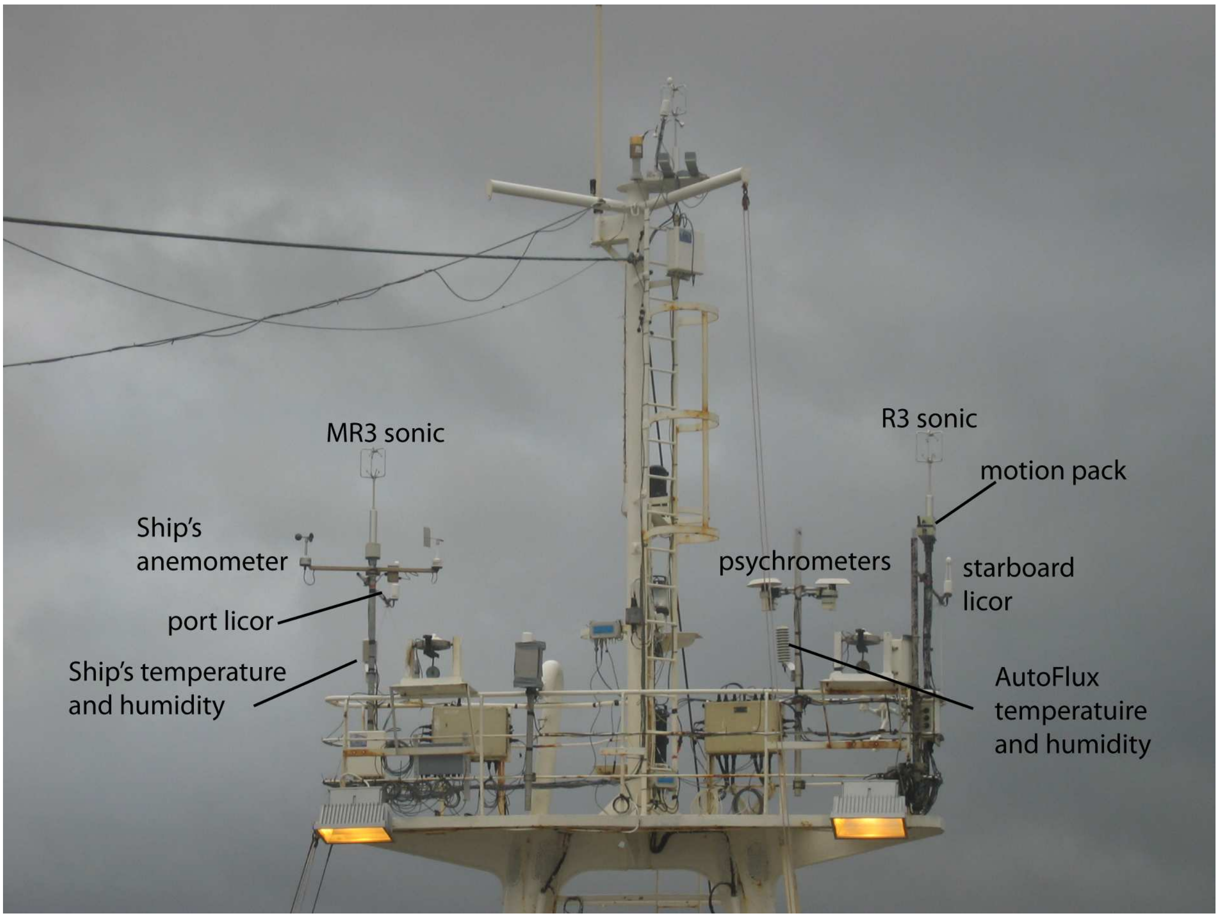

Figure 26.1a. The meteorological sensors on the foremast platform of the RRS *Discovery*.

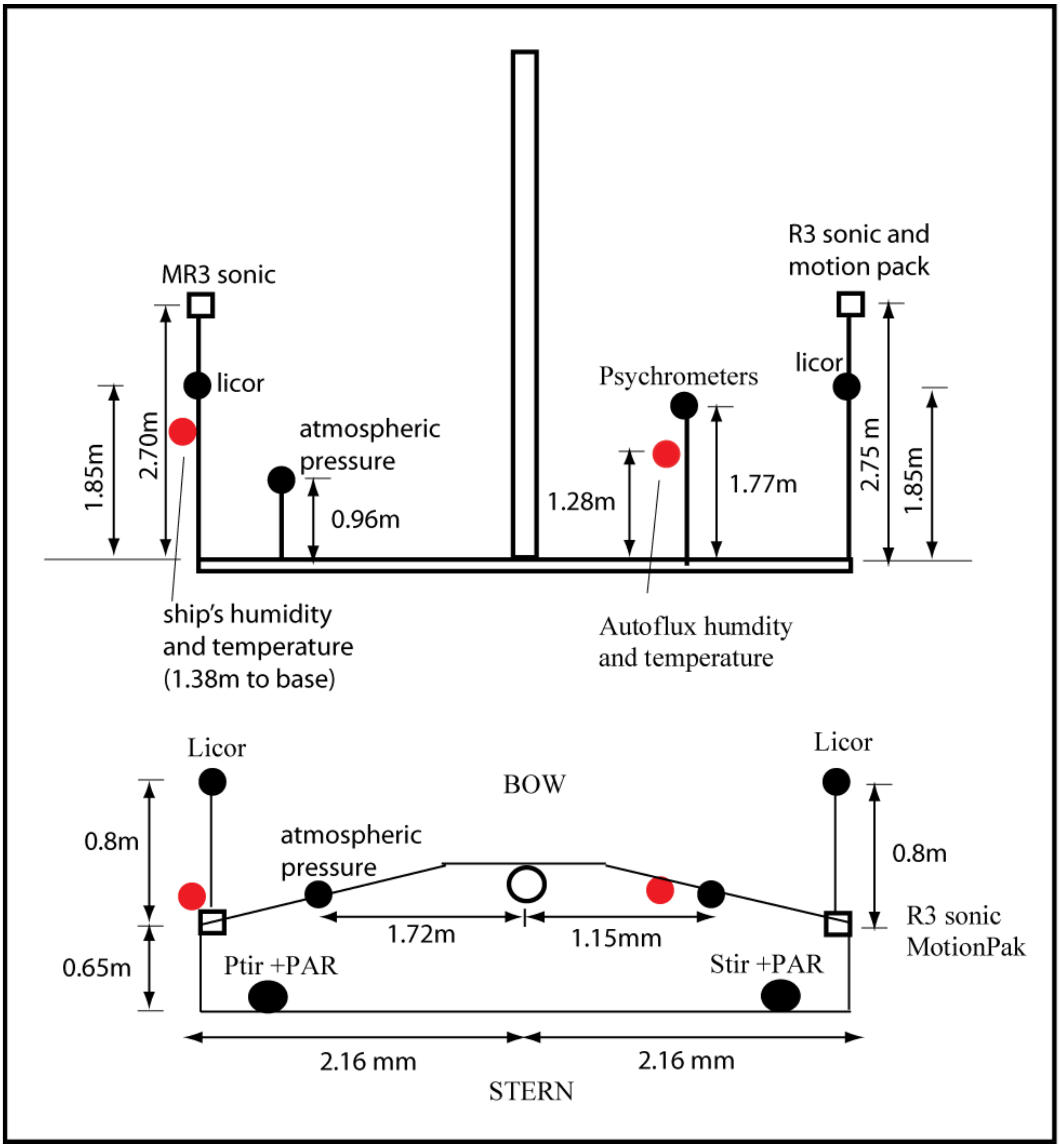

-

Figure 26.1b. Schematic plan view of the foremast platform, showing the positions of the sensors. Heights are from the centre of the sensor volume above the platform.

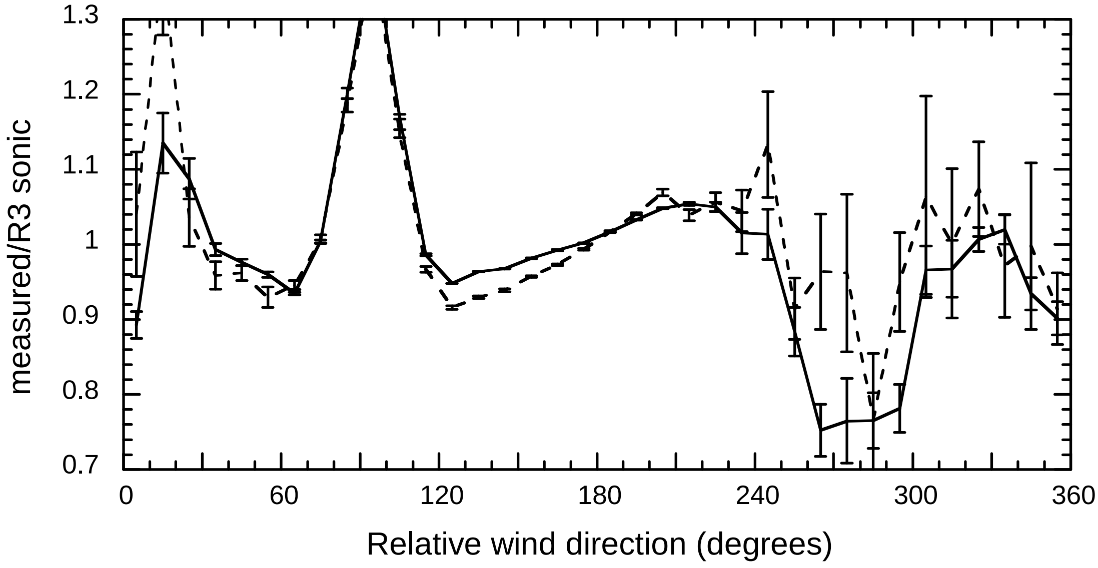

Figure 26.2. Measured wind speed / wind speed from the R3 sonic, MR3 sonic (bold line) and ship's anemometer (dashed line) each binned against relative wind direction. Only open ocean data is displayed and error bars indicate the standard deviation of the mean. A relative wind direction of 180 degrees indicates a flow directly on to the bow of the ship.

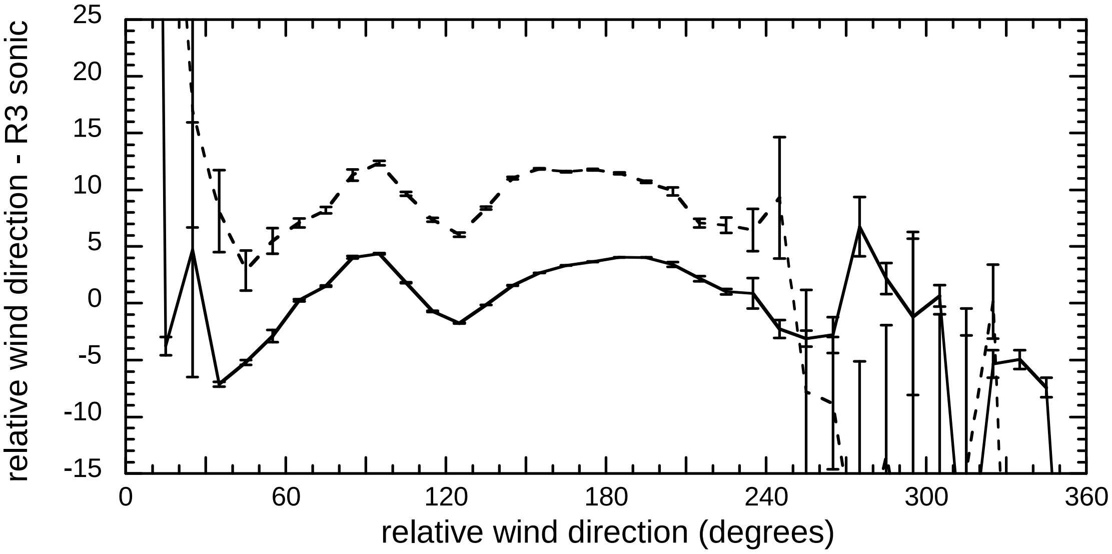

Figure 26.3. As Figure 26.2 but showing the difference (measured – R3 sonic) in the relative wind direction.

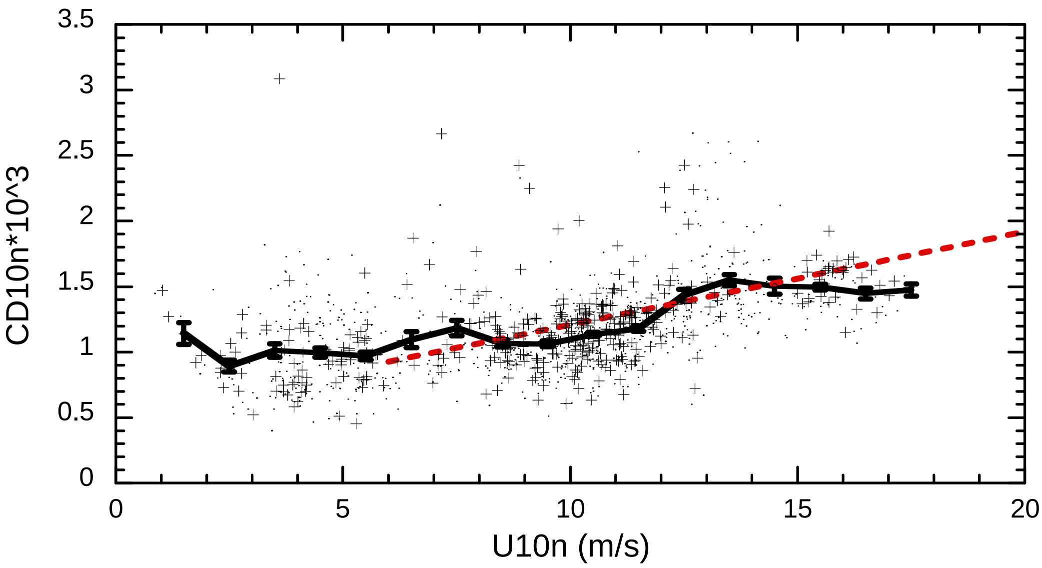

Figure 26.4. Fifteen minute averaged values of the measured Inertial Dissipation drag coefficient from the R3 sonic (dots) and the MR3 sonic (crosses), plus the mean results of both instruments (solid line) binned against the 10 m neutral wind speed. The Yelland et al. (1998) relationship is shown by the dashed line.

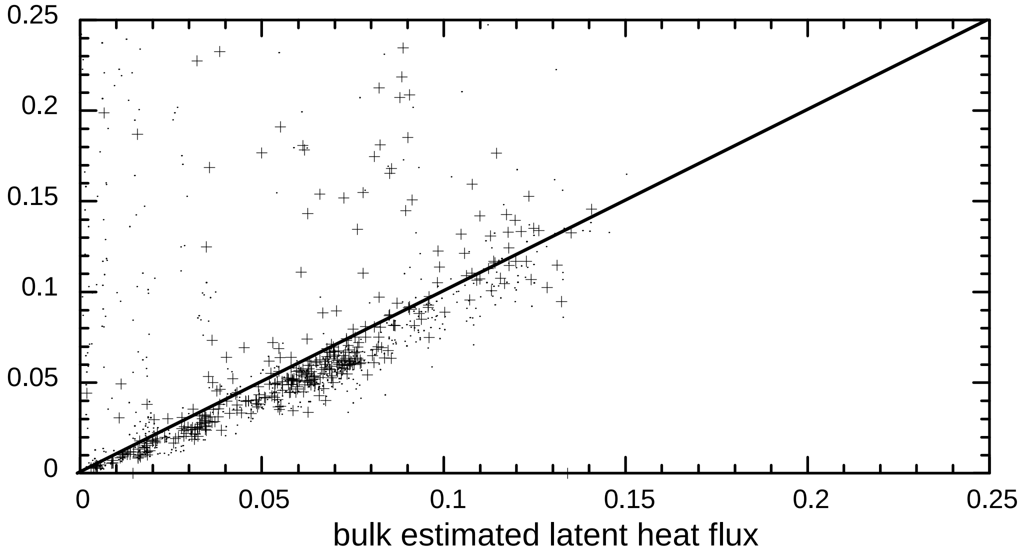

Figure 26.5. Inertial dissipation (ID) measurements of the kinematic latent heat flux from starboard Licor (dots) and the port Licor (crosses) shown against a flux estimated from a bulk formula (Smith, 1988).

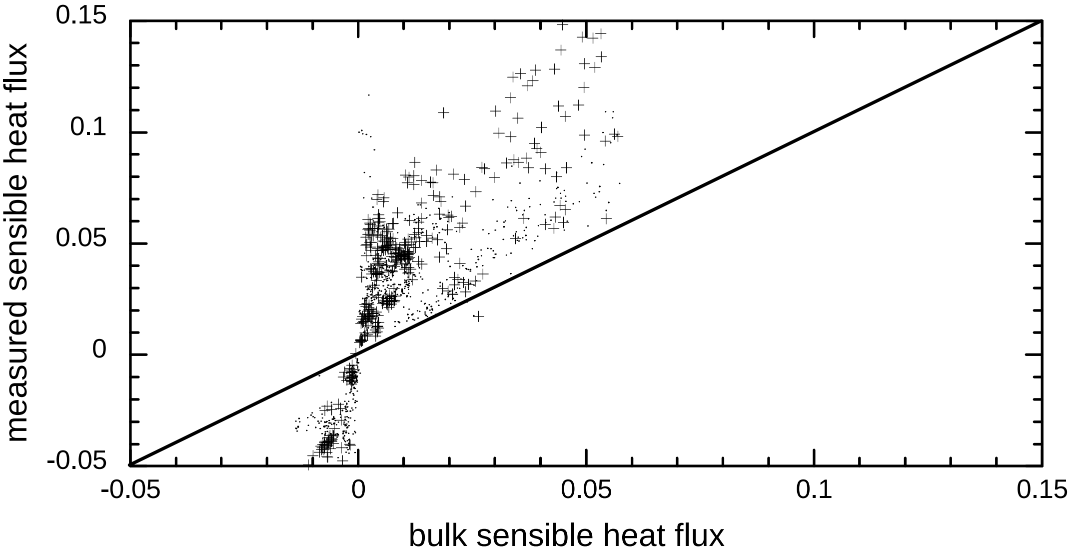

Figure 26.6. Inertial dissipation (ID) measurements of the kinematic sensible heat flux from the R3 Sonic (dots) and the MR3 sonic (crosses) shown against a flux estimated from a bulk formula (Smith, 1988).

Appendix A. List of significant events.

Day 96-98: Autoflux system hung. No summary data received over Iridium so the ship was contacted and Ian Brooks rebooted the UNIX box.

Licor cleaned	TIR sensors cleaned
Jday 079 13:40	Jday 079 13:45
Jday 102 11:00	Jay 102 11:00

Table A.1. Day and time when sensors were cleaned.

Appendix B. Time series of mean meteorological and air-sea flux data.

The following Figures show time series of 1 minute averages of the mean meteorological data. Only basic quality control criteria have been applied to these data. Each page contains four plots showing different variables over a five day period.

Top panel - the best wet (pwUSE) and dry (pdUSE) bulb temperatures from the two psychrometers plus sea surface temperature (SST) from the TSG.

Upper middle panel – down-welling radiation from the two shortwave TIR sensors in W/m^2.

Lower middle panel - relative wind direction (reldd = 180 degrees for a wind on the bow) and true wind direction (TRUdd) from the starboard R3 anemometer. The ship's true heading is also shown.

Bottom panel - relative (spdENV) and true wind (TRUspd) speeds in m/s from the starboard R3 anemometer. The ship's speed over the ground is also shown in m/s. When the relative wind direction was to port of the bow the significant flow distortion is apparent as steps in the true wind speed.

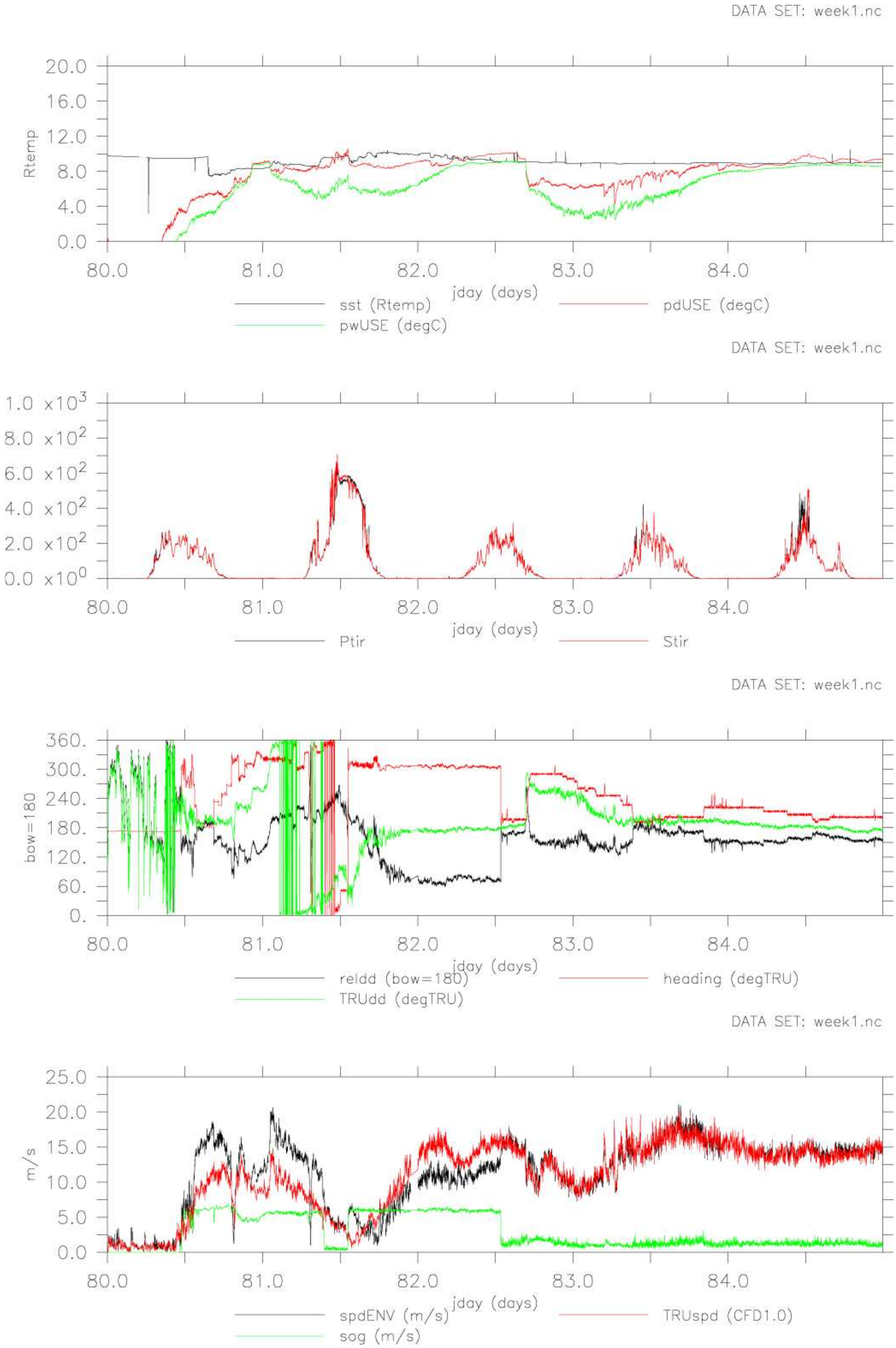

Figure 27.1. Mean meteorological data for days 80 to 85.

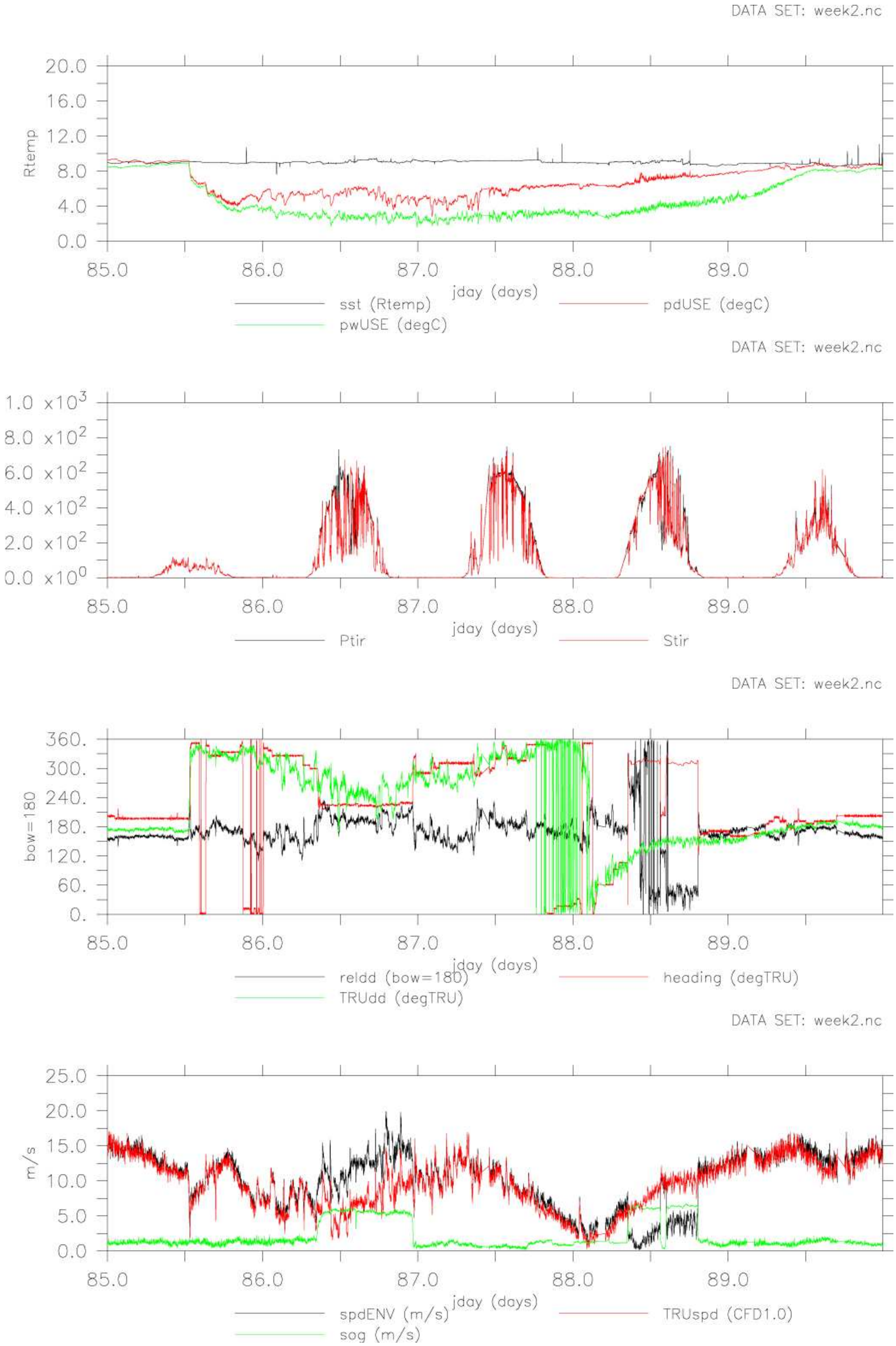

Figure 27.2. Mean meteorological data for days 85 to 90.

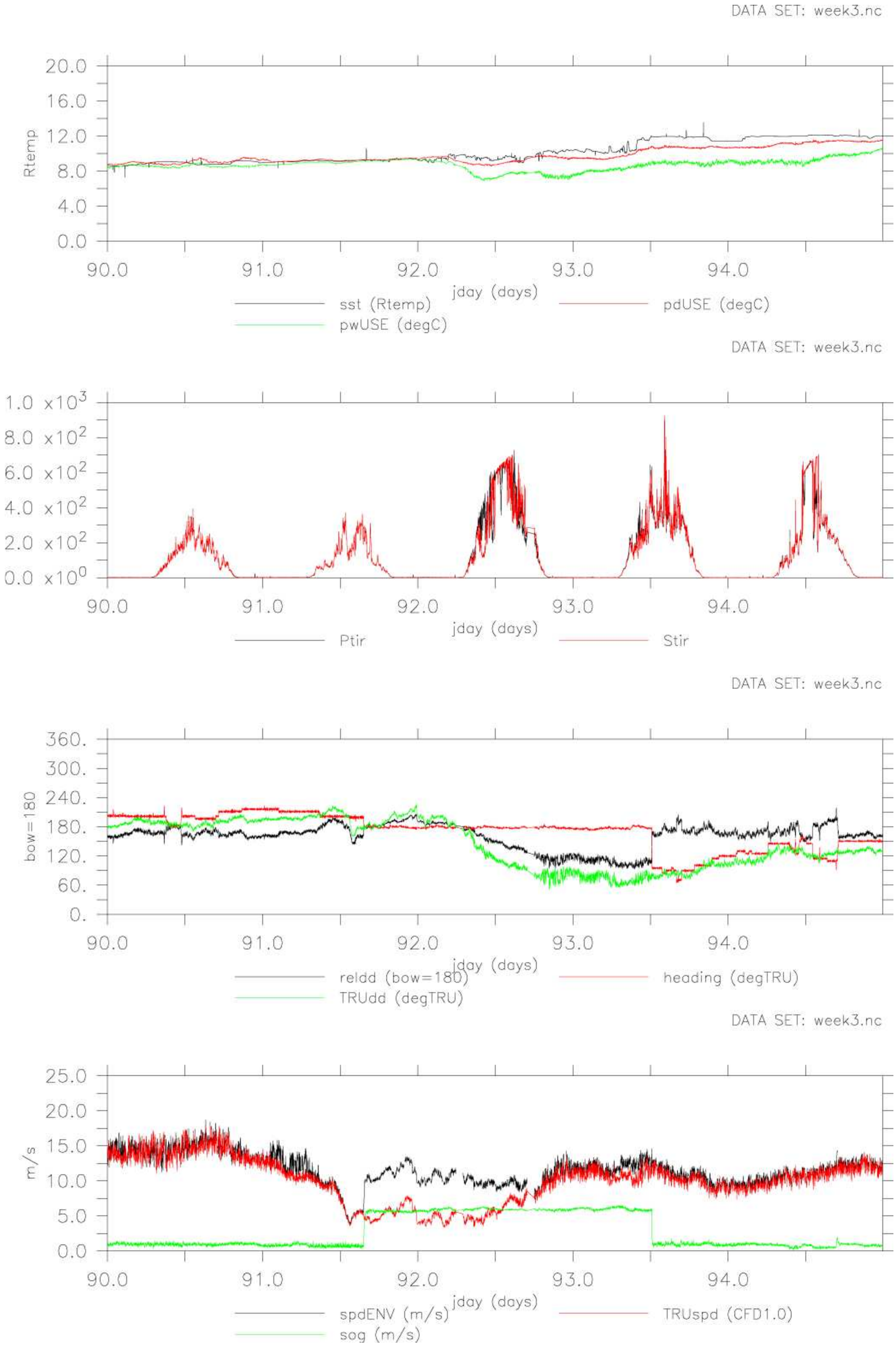

Figure 27.3. Mean meteorological data for days 90 to 95.

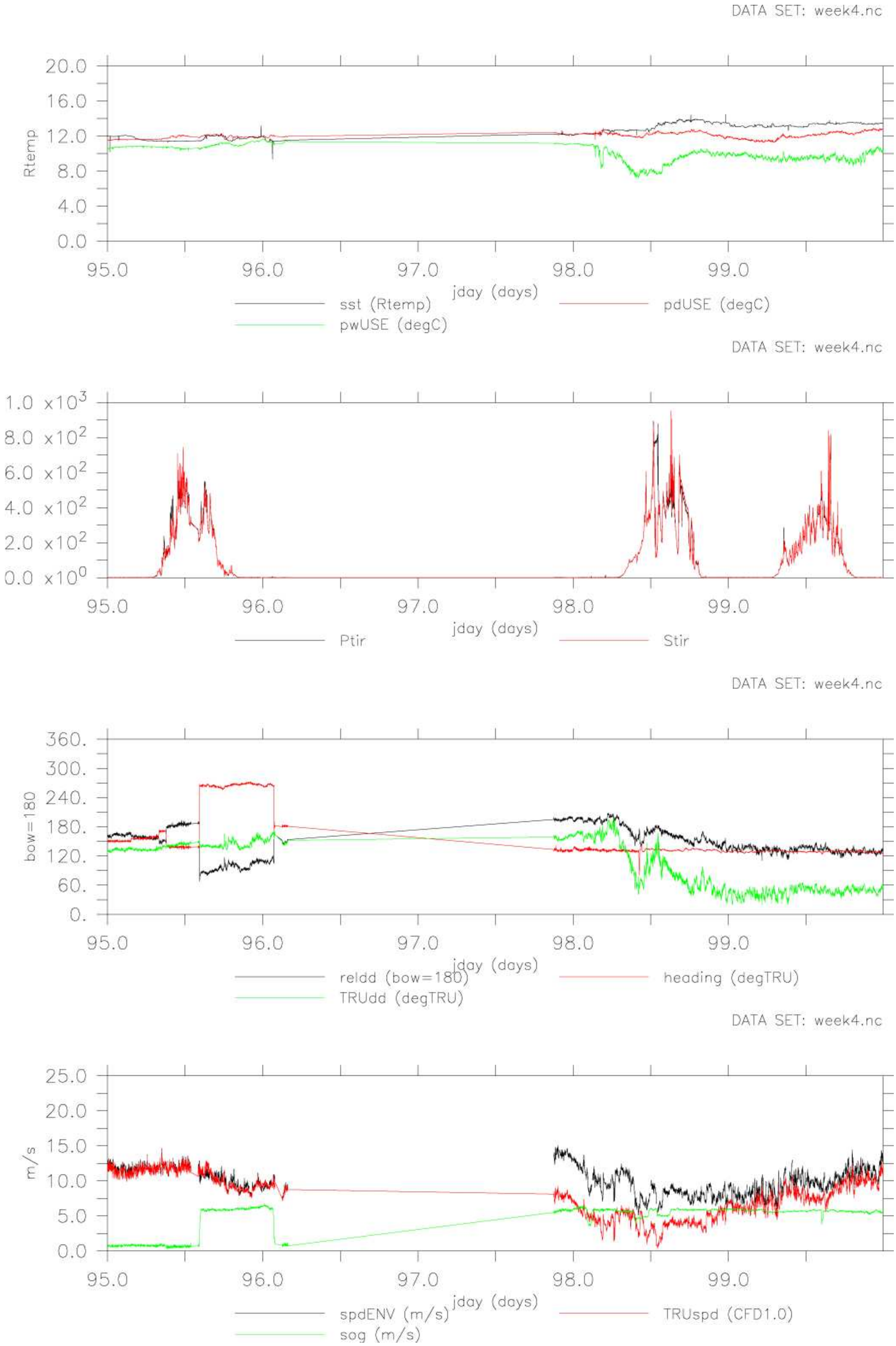

Figure 27.4. Mean meteorological data for days 95 to 100.

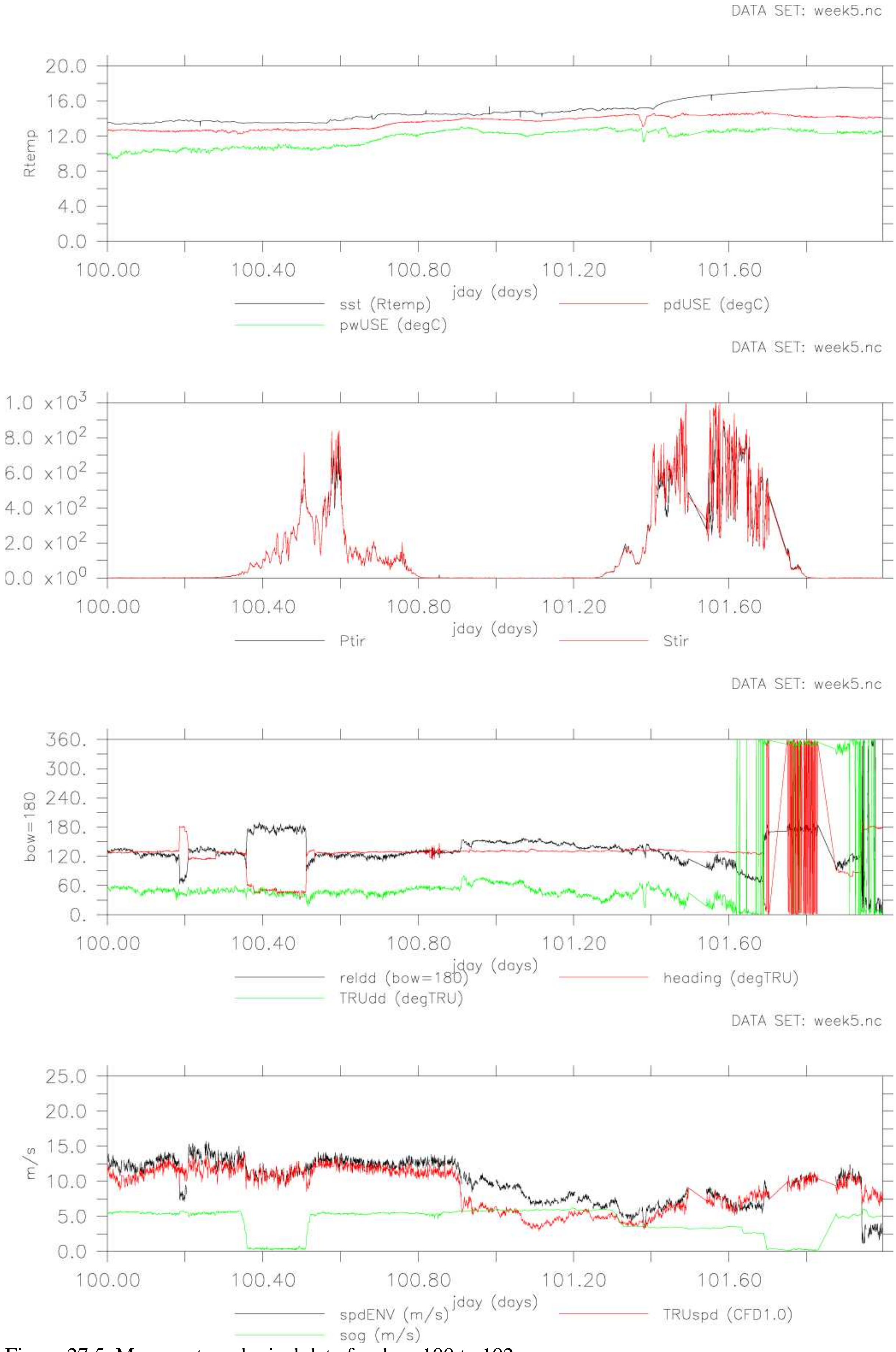

Figure 27.5. Mean meteorological data for days 100 to 102.

2. Whitecapping Cameras (Ian Brooks and Ben Moat)

2.1 Introduction

Two Nikon Coolpix 8800 cameras were installed on the bridge to measure the whitecap fraction of breaking waves at the sea surface. The cameras were located on the port side of the bridge at a height of 13 m above the sea surface. Both cameras were set at an angle of 22 degrees from the horizontal so that the top of the image was set to the horizon. Images were taken directly abeam every 30 seconds during daylight hours and recorded to internal 2 Gb flash cards. The camera resolutions were set at 3Mpixels and 5Mpixels for the front and rear cameras respectively (Figure 28.1). During the cruise the cameras had to be checked frequently due to both cameras randomly 'freezing'. Post cruise this problem was identified as a dirty power supply (unsmoothed supply) from a 240V socket on the bridge. A clean power supply was identified post cruise and used during the DOGEE II cruise D320 in June 2007. The cameras generated about 2.5Gb of data per day, which was transferred to an external disk and the ships UNIX systems daily.

2.2 Data Processing

The basic assumption is that for each image all pixels with red, green and blue (RGB) levels above a certain threshold value correspond to whitecaps, and all other elements in the image having RGB levels below that threshold correspond to non-whitecap areas (Figure 28.2). It is relatively straightforward to determine the threshold value by visually inspecting each image in turn using image-processing software. Unfortunately it is impractical to do this for the 80,000 images collected from both cameras during the cruise. Matlab scripts developed to calculate the whitecap fraction during a previous SOLAS cruise (Upstill-Goddard et al. 2007) will be applied to the D317 data post cruise. Figure 28.2 shows the script applied to an image taken on Jday 90.

Figure 28.1 Digital cameras installed on the port side of the bridge to take images of the sea surface abeam of the ship.

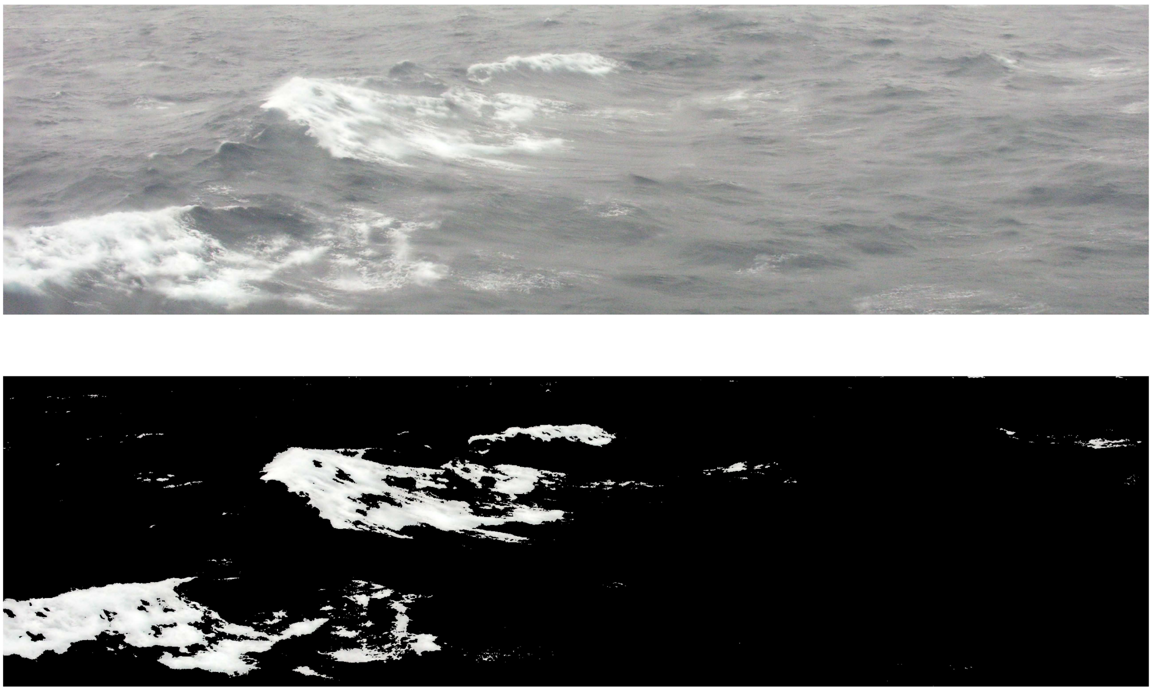

Figure 28.2 a) An image of the sea surface taken by the rear bridge camera during Jday 90 and b) the corresponding processed white cap image.

References

Upstill-Goddard R. (and Co-authors), 2007: DOGEE-SOLAS and SEASAW; high wind gas and aerosol fluxes in the North East Atlantic Ocean, UK-SOLAS Cruise Report: RRS Discovery Cruise D313, 07 November - 06 December, 2006, BODC, Liverpool, UK, 109 pp.
www.bodc.ac.uk/data/information_and_inventories/cruise_inventory/report/d313.pdf

PML autonomous measurement of pCO_2 on D317

Nick Hardman-Mountford

The partial pressure of CO_2 (pCO_2) in marine air and seawater was measured by the PML/Dartcom autonomous pCO_2 measurement system installed in the chemistry laboratory of Discovery. The system uses an equilibrator to extract gaseous CO2 from seawater. Seawater is supplied to the equilibrator from the non-toxic seawater supply. Marine air is sampled from the monkey island. Both air streams are dried and the CO_2 content measured using a non-dispersive infra-red analyser. Three standard gases of known CO_2 content (0, 250 and 450 ppm) were also sampled to calibrate against drift of the infra-red analyser. The pCO_2 system was set up to sample in the following sequence: equilibrator air, marine air, standard gases, with a total cycle length of 58 minutes. The system was looked after onboard by Martin Bridger and Leighton Rolley from NERC NMF SeaSystems. They cleaned the equilibrator prior to departure. No problems have been noted in the operation of the pCO_2 measurement system, although problems with iridium satellite communications resulted in data only being periodically communicated back to PML via the ship's e-mail systems. The ancillary data streams necessary for post-processing of pCO_2 data: (inlet (hull) temperature, conductivity, TSG temperature, calculated salinity, atmospheric pressure) were not configured for integration to the pCO_2 system data file so these were obtained from the ship's Surfmet system after the cruise.

The full set of logged cruise data have undergone preliminary processing by Nick Hardman-Mountford from PML following the cruise (figure 29), however calibration offsets for equilibrator temperature sensors, the ship's underway temperature sensors still need to be applied, together with CTD station temperature and salinity corrections. The data processing uses Weiss & Price (1980) for humidity corrections, Takahashi et al. (1993) for equilibrator temperature corrections and Weiss et al. (1974) for the virial coefficients when calculating fugacity.

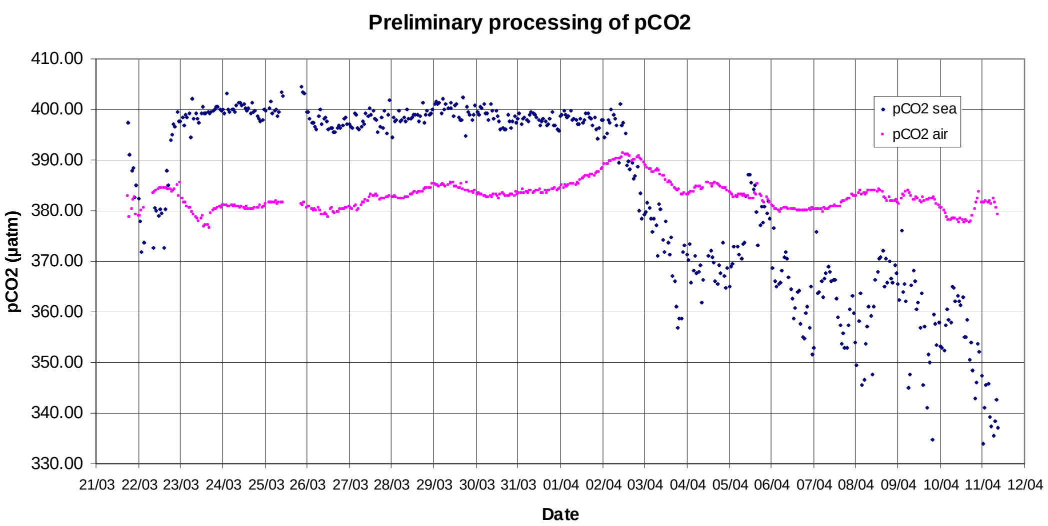

Figure 29. pCO2 data after preliminary processing.

REFERENCES

Andreas, E. L. and K. Emanuel (2001) Effects of sea spray on tropical cyclone intensity. *J. Atmos. Sci.* **58**, 3741-3751.

AutoFlux group, 1996: AutoFlux - an autonomous system for monitoring air-sea fluxes using the inertial dissipation method and ship mounted instrumentation. Proposal to MAST research area C - Marine Technology, 38 pp. + appendices

Edson, J. B. A. A. Hinton, K. E. Prada, J. E. Hare, and C. W. Fairall, (1998), Direct covariance flux estimates from mobile platforms at sea, *J. Atmos. Oceanic, Technol.*, *15*, 547-562.

Geever, M. C. D. O'Dowd, S. van Ekeren, R. Flanagan, E. D. Nilsson, G. de Leeuw, Ü. Rannik, (2005), Submicron sea spray fluxes, *Geophys. Res. Lett. 32*, doi: 10.1029/2005GL023081.

Haywood J. et al. 1999: Tropospheric aerosol climate forcing in clear-sky satellite observations over the oceans. Science, 283.

Hill, M. K., B. J. Brooks, S. J. Norris, M. H. Smith, I. M. Brooks, G. de Leeuw, and J. J. N. Lingard, (2007), CLASP: A novel fast response particle spectrometer, *J. Atmos. Oceanic. Tech.* (submitted).

McGillis, W. R., J. B. Edson, J. D. Ware, J. W. H. Dacey, J. E. Hare, C. W. Fairall, and R. Wanninkhof (2001b), Carbon dioxide flux techniques performed during GasEx-98, Mar. Chem., 75, 267– 280.

Nilsson, E. D., Ü. Rannik, E. Swietlicki, C. Leck, P. P. Aalto, J. Zhou, and M. Norman, (2001), Turbulent aerosol fluxes over the Arctic Ocean: 2. Wind driven sources from the sea. *J. Geophys. Res.*, *106*, 32,139-32,154.

Norris, S. J., I. M. Brooks, G. de Leeuw, M. H. Smith, M. Moeman, J. J. N. Lingard, (2007), Eddy covariance measurements of sea spray particles over the Atlantic Ocean, *Atmos. Chem. Phys.* (submitted)

Smith, S. D., 1988: Coefficients for Sea Surface Wind Stress, Heat Flux and Wind Profiles as a Function of Wind Speed and Temperature. *J. Geophys. Res.*, **93**, 15467-15474.

Takahashi, T., Feely, R.A., Weiss, R., Wanninkhof, R.H., Chipman, D.W., Sutherland, S.C., Takahashi, T.T., 1997. Global air–sea flux of CO2: an estimate based on measurements of sea–air pCO2 difference. Proceedings of the National Academy of Science 94, 8292–8299.

Taylor, P. K., M. J. Yelland, R. W. Pascal, B. I. Moat, I. Skjelvan, C. C. Neill, (2007), Determining the magnitude of the CO_2 flux over the ocean. *Geophys. Res. Lett.*, SUBMITTED.

O'Dowd, C. D., J. A. Lowe, and M. H. Smith, 1999: Coupling of sea-salt and sulphate interactions and its impact on cloud droplet concentration predictions, Geophy. Res. Lett., 26, (9), 1311-1314.

O'Dowd, C. D., J. A. Lowe, N. Clegg, M. H. Smith, and S. L. Clegg, 2000: Modeling heterogeneous sulphate production in maritime stratiform clouds. J. Geophys. Res. 105, D6, 7143 – 7160.

Yelland, M. J., P. K. Taylor, I. E. Consterdine, and M. H. Smith, 1994: The use of the inertial dissipation technique for shipboard wind stress determination, *J. Atmos. Oceanic Technol.*, 11, 1093-1108

Yelland, M. J., B. I. Moat, P. K. Taylor, R. W. Pascal, J. Hutchings and V. C. Cornell, 1998: Wind stress measurements from the open ocean corrected for airflow disturbance by the ship. *J. Phys. Oceanogr.,* **28**, 1511 - 1526.

Yelland, M. J., B. I. Moat, R. W. Pascal and D. I. Berry, 2002: CFD model estimates of the airflow distortion over research ships and the impact on momentum flux measurements. *J. Atmos. Oceanic Technol*. 19, 1477-1499.